Innovative Food Science and Emerging Technologies 19 (2013) 15–28

Contents lists available at SciVerse ScienceDirect

Innovative Food Science and Emerging Technologies

journal homepage: www.elsevier.com/locate/ifset

Advanced applications of hyperspectral imaging technology for food quality and safety analysis and assessment: A review — Part II: Applications

Di Wu, Da-Wen Sun *

Food Refrigeration and Computerised Food Technology (FRCFT), School of Biosystems Engineering, University College Dublin, National University of Ireland, Agriculture & Food Science Centre, Belfield, Dublin 4, Ireland

ARTICLE INFO

Article history:
Received 23 February 2012
Accepted 21 April 2013

Editor Proof Receive Date 6 June 2013

Keywords:
Hyperspectral imaging
Imaging spectroscopy
Food quality
Food safety
Meat
Fruit
Vegetable
Spectrometry

ABSTRACT

In recent years, hyperspectral imaging has gained a wide recognition as a non-destructive and fast quality and safety analysis and assessment method for a wide range of food products. As the second part of this review, applications in quality and safety determination for food products are presented to illustrate the capability of this technique in the food industry for classification and grading, defect and disease detection, distribution visualization of chemical attributes, and evaluations of overall quality of meat, fish, fruits, vegetables, and other food products. The state of the art of hyperspectral imaging for each of the categories was summarized in the aspects of the investigated quality and safety attributes, the used systems (wavelength range, acquisition mode), the data analysis methods (feature extraction, multivariate calibration, variables selection), and the performance (correlation, error, visualization). With its success in different applications of food quality and safety analysis and assessment, it is evident that hyperspectral imaging can automate a variety of routine inspection tasks.

Industrial relevance: It is anticipated that real-time food monitoring systems with this technique can be expected to meet the requirements of the modern industrial control and sorting systems in the near future.

Contents

1. Introduction

Nowadays, quality and safety becomes a key factor for the modern food industry, because consumers always prefer food products with superior quality at an affordable price. It is a big concern to analyze and assess quality and safety attributes of food products in all processes of the food industry. Recently, with the integration of two mature technologies of imaging (Sun and Brosnan, 2003; Du and Sun, 2005; Jackman, Sun, Du and Allen, 2008; Sun, 2008a) and spectroscopy (Sun, 2008b), hyperspectral imaging technique has been investigated as a potential analytical tool for non-destructive analysis and assessment for food quality and safety. In the first part of this review, some fundamental knowledge about hyperspectral imaging is introduced. As the second part, this paper introduces recent investigative and exploratory studies in major areas that have been impacted by this technique including meat, fruit and vegetables, grains, and others. Several reviews and books on application of

* Corresponding author. Tel.: +353 1 7167342; fax: +353 1 7167493.
E-mail address: dawen.sun@ucd.ie (D.-W. Sun).
URL: http://www.ucd.ie/refrig, http://www.ucd.ie/sun (D.-W. Sun).

1466-8564/$ – see front matter © 2013 Elsevier Ltd. All rights reserved.
http://dx.doi.org/10.1016/j.ifset.2013.04.016

hyperspectral imaging in food quality assessment have already been published in the last years (Gowen, O'Donnell, Cullen, Downey, & Frias, 2007; Lorente et al., 2012; Nicolai et al., 2007; Sun, 2010). Therefore, more attention is given in this review to the applications since 2010.

2. Quality and safety analysis and assessment of meat and meat products

Production of high quality meat and meat products is important for the modern meat industry. Superior quality of these products is always demanded by consumers and is considered as a key factor for success in today's highly competitive market.

As the most important factor in consumer perception of beef palatability or quality, tenderness is the widely discussed and most relevant quality characteristic of beef, and its assessment in meat has been investigated in some researches since 2008 (Elmasry & Sun, 2010). Recently, Wu et al. (2010) obtained a better correlation coefficient of 0.86 for WBSF determination using hyperspectral scattering imaging technique and they further improved the correlation coefficient into 0.91 (Wu et al., 2012d). In the same group, the same hyperspectral scattering imaging system with the spectral range of 400–1100 nm was also investigated for the determination of the tenderness of pork (Tao, Peng, Li, CHao, & Dhakal, 2012). The highest correlation coefficient for cross validation (r_{cv}) of 0.930 was obtained by using the parameter (b–a)/c, where a was asymptotic value, b was peak value, and c was full width at b/2. In addition, important wavelengths in the spectral region of 900–1700 nm were identified as the inputs to establish partial least squares regression (PLSR) models for the WBSF determination of beef (ElMasry, Sun, & Allen, 2012) and lamb (Kamruzzaman, ElMasry, Sun, & Allen, 2013), resulting in good prediction results with coefficient of determination (r^2) of 0.83 and r of 0.84, respectively.

Water is the major component in food (Delgado and Sun, 2002) and agricultural products (Sun and Woods, 1993, 1994a, 1994b, 1994c, 1997; Sun and Byrne, 1998, Sun, 1999), and it is a routine task to analyze water content or moisture content. In meat and meat products, water is omnipresent, and its determination is frequently required for meat industry. A hyperspectral imaging system in the range of 900–1700 nm was applied to determine water content of lamb (Kamruzzaman, ElMasry, Sun, & Allen, 2012), pork (Barbin, ElMasry, Sun, & Allen, 2012), beef (ElMasry, Sun, & Allen, 2013), pre-sliced turkey hams (Iqbal, Sun, & Allen, 2013), and Spanish cooked ham (Talens et al., 2013). On the basis of feature wavelengths, the PLSR models were established in these works. The output results showed a good water prediction ability of hyperspectral imaging for lamb (coefficient of determination for prediction (r_p^2) of 0.88), pork (r_p^2 of 0.87), beef (r_p^2 of 0.89), pre-sliced turkey ham (r_{cv}^2 of 0.88), and Spanish cooked ham (r_{cv}^2 of 0.868). Besides water content, water holding capacity (WHC), which is commonly measured as drip loss, is another water related attribute not only for food-processing industry but also for consumers during purchasing meat (Prevolnik, Candek-Potokar, & Skorjanc, 2010). Hyperspectral imaging in the range of 900–1700 nm has been applied to determine WHC/drip loss in beef, pork, and lamb meats (Barbin, ElMasry, Sun, & Allen, 2012; ElMasry, Sun, & Allen, 2011; Kamruzzaman, ElMasry, Sun, & Allen, 2012). Six and seven important wavelengths were selected for beef and pork analysis. Although the wavelength selections were conducted for different meats, there were some wavelengths selected for both beef and pork, such as 940 nm, 990/997 nm, and 1208/1214 nm. On the basis of the selected important wavelengths, the new PLSR models were built and led to r_{cv}^2 of 0.87 and 0.83 for beef and pork, respectively. In addition, long-wave near infrared spectral region had a better ability in predicting drip loss of pork ($r^2_{cv} = 0.83$ vs. $r = 0.77$) (Barbin et al., 2012c; Qiao et al., 2007).

Fat is an important quality criteria for the production controls from slaughter to final product in the meat industry. In the last two years, hyperspectral imaging has been used for the prediction of fat content in meats. In the short-wave near infrared spectral region (760 to 1040 nm), interactance imaging technique was applied for on-line measurement of fat content in inhomogeneous beef (Wold, O'Farrell, Hoy, & Tschudi, 2011) and pork trimmings (O'Farrell, Wold, Hoy, Tschudi, & Schulerud, 2010). The calibration model had a very predictive performance for on-line determination of the fat content of beef trimmings ($r = 0.98$, root mean square error of cross-validation (RMSECV) = 3.0%). When long-wave near infrared spectral region, was considered, a pushbroom hyperspectral imaging system in the reflectance mode (900–1700 nm) was used as a fast and non-destructive determination method of fat content in intact and minced pork (Barbin et al., 2012b), lamb (Kamruzzaman et al., 2012b) beef (ElMasry et al., 2013), and cooked ham (Talens et al., 2013). Good r^2 of 0.95, 0.91 and 0.89 was obtained by cross-validated PLSR models for pork, lamb, and beef analysis, respectively, while the prediction of cooked ham was not very good ($r^2 = 0.369$). In another study, hyperspectral images with broader range of 1000–2300 nm were acquired for the determination of total fat in beef cuts with good prediction abilities (r^2 of 0.90) (Kobayashi, Matsui, Maebuchi, Toyota, & Nakauchi, 2010). Besides assessing fat content, hyperspectral imaging has also been used for determining the proportions of total saturated fatty acid (SEA), total unsaturated fatty acid (UFA), and the main fatty acids of myristic (C14:0), palmitic (C16:0), stearic (C18:0), myristoleic (C14:1), palmitoleic (C16:1), oleic (C18:1) and linoleic (C18:2) in beef cuts (Kobayashi et al., 2010). The results obtained from these studies clearly revealed that hyperspectral imaging can be used for the non-destructive prediction of fat content in meats.

Meat products with contaminants have the capability of causing illness in humans, when no automatic inspection protocols but only human vision detection is in operation during slaughter and processing. The pioneer research of utilizing hyperspectral and multispectral imaging techniques for the determination of different contaminants on poultry carcasses is conducted in the last decade by the USDA's Agricultural Research Service, and some of these systems have already been set up in online monitoring line (Elmasry & Sun, 2010). Recently, a prototype line-scan hyperspectral imaging system was developed by Yoon, Park, Lawrence, Windham, and Heitschmidt (2011) for online detection of surface fecal material and ingesta (Fig. 1). An off-the-shelf hyperspectral image camera was integrated into the system with two line lights and a custom software program for real-time imaging. Multithreaded software architecture was designed and implemented for the data acquisition, which is the bottleneck of the imaging system. The study found that the system could grab and process three waveband images of carcasses moving up to 180 birds per minute (a line-scan rate 286 Hz) and detect fecal material and ingesta on their surfaces. The detection accuracy of the system varied between 89% and 98% with minimum false positive errors (less than 1%), depending on tested detection algorithms (Yoon et al., 2011). In other studies, an online wholesomeness inspection system was developed for differentiation of wholesome and systemically diseased chickens on a high-speed processing line with a speed of 140 bird/min (Chao, Yang, & Kim, 2010; Yang et al., 2010). An effective multispectral inspection could be achieved by analysis of a selected region of interest across the breast area from images at the 580 and 620 nm wavebands, which provide the greatest difference between the average wholesome and average unwholesome chicken spectra.

Besides contamination detection, in recent years, the research on food safety inspection using hyperspectral imaging has been extended in the area of microbial spoilage detection. In recent years, the feasibility of hyperspectral imaging for total viable count (TVC) determination of pork meat has been investigated (Tao et al., 2010; Wang, Peng, Huang, & Wu, 2011; Wang, Peng, & Zhang, 2010). Least squares support vector machine (LS-SVM) was found to have better ability for establishing the quantitative relationship between spectral data of

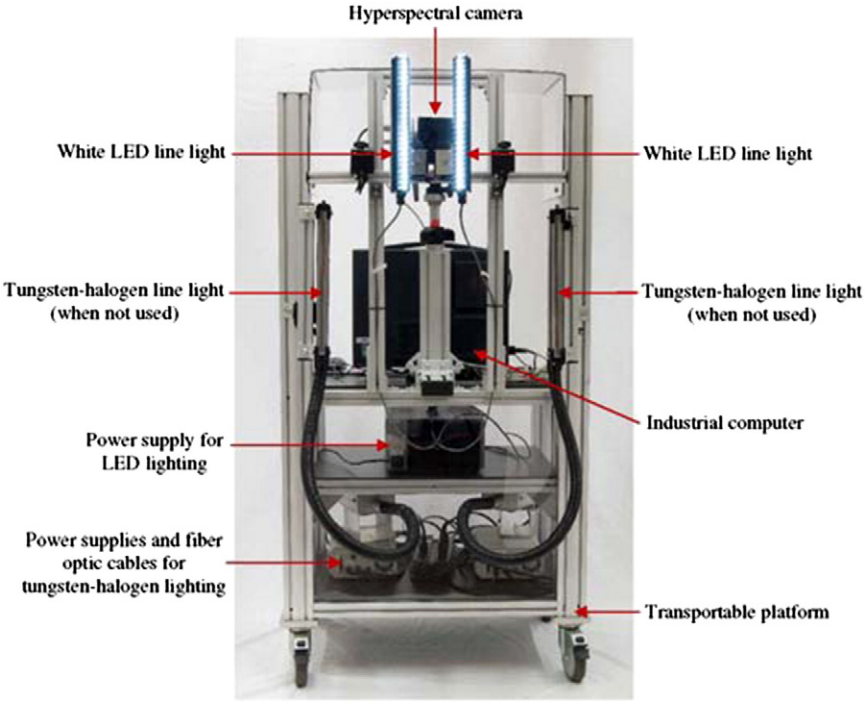

Fig. 1. Overview of the prototype line-scan hyperspectral imaging system for real-time inspection of poultry carcasses with fecal material and ingesta (Yoon et al., 2011).

samples and their TVC values, than other methods, such as multiple linear regression (MLR), PLSR, and artificial neural networks (ANN). Hyperspectral imaging has also been used for the microbial spoilage determination of chicken filets, such as TVC (Feng & Sun, 2012), *Pseudomonas* (Feng & Sun, 2013), and Enterobacteriaceae (Feng, ElMasry, Sun, Walsh, & Morcy, 2012), and porcine meat, such as TVC and psychrotrophic plate count (PPC) (Barbin, ElMasry, Sun, Allen, & Morsy, 2012). When the hyperspectral scattering imaging was used for the determination of TVC of beef, a very good result with $r^2 = 0.95$ and SEP = 0.30 was obtained by the established PLSR model based on three combinations of scattering parameters (i.e. a, b and a × b) (Peng et al., 2011). Later, different from the previous researches on detecting TVC, hyperspectral scattering technique was applied for the specific determination of pork *Escherichia coli* (*E. coli*) contamination (Tao et al., 2012). Three parameters of a (asymptotic value), b (peak value) and c (full width at b/2) were obtained by using Lorentzian distribution function to fit the scattering profiles. High correlation coefficients of 0.877 and 0.841 were obtained using parameters of a and "a&b&c", respectively. In comparison, the results for prediction of TVC during meat storage using hyperspectral scattering technique are better than that for predicting *E. coli* contamination, specifically. More works should be conducted on determining specific bacterial spoilages in meat.

In addition to the above quality and safety attributes, in recent years, hyperspectral imaging has also been investigated for determination of other meat qualities, such as color parameters (L^*, a^*, b^*), pH, and protein. Color is the first quality attribute of food evaluated by consumers, and is therefore an important component of food quality relevant to market acceptance (Wu & Sun, 2012). Besides color, pH is another important physical characteristic of meat. All papers using hyperspectral imaging with the wavelength range of 900–1700 nm for color and pH prediction were published. In all four works including beef (ElMasry et al., 2012), pork (Barbin et al., 2012c), lamb (Kamruzzaman et al., 2012c), and sliced turkey hams (Iqbal et al., 2013), the method of weighted regression coefficients was applied to select important wavelengths. On the basis of selected wavelengths, the L^* and pH values were predicted with r^2_{cv} of 0.88 and 0.75 for beef, 0.93 and 0.87 for pork, 0.91 (L^*) for lamb, and 0.81 (pH) for sliced turkey hams, respectively. It is noticed that compared to previous work (Qiao et al., 2007) which used the wavelengths between 400 and 1000 nm, the wavelength range of 900–1700 nm showed better determination ability of color and pH of meat. In addition to L^*, Barbin et al. (2012c) also investigated the determination of other color parameters, such as a^* ($r^2_{cv} = 0.75$), b^* ($r^2_{cv} = 0.89$), Chroma ($r^2_{cv} = 0.83$), and Hue angle ($r^2_{cv} = 0.87$). However, the determination of a^* of beef was not satisfactory, when the hyperspectral imaging with reflectance mode was applied (ElMasry et al., 2012). Differently, the hyperspectral imaging with scattering mode showed good prediction abilities for determining not only color parameters (L^*, b^*) and pH like the reflectance mode, but also color parameter (a^*) of beef (correlation coefficients of 0.90 and 0.96, respectively) (Wu et al., 2010; Wu et al., 2012d). In addition, NIR hyperspectral imaging in tandem with PLSR modeling also showed reasonable good prediction performance for protein in lamb (Kamruzzaman et al., 2012b), pork (Barbin et al., 2012b), beef (ElMasry et al., 2013), and Spanish cooked ham (Talens et al., 2013).

The above mentioned quality and safety attributes were those generally measured by chemical manipulations or instrumental methods. Besides, sensory analysis is also commonly used in evaluating meat quality based on human senses (sight, smell, taste, touch and hearing). Some works have been carried out to estimate the feasibility of using hyperspectral imaging to predict sensory attributes of meat products, such as tenderness, juiciness, flavor, and overall acceptability (Barbin et al., 2012c; Kamruzzaman, ElMasry et al., 2013). The results revealed that the attributes of flavor and overall acceptability could not be properly predicted based on the hyperspectral reflectance images in the wavelength range of 900–1700 nm, while juiciness of pork ($r^2_{cv} = 0.49$) and tenderness of pork ($r^2_{cv} = 0.54$) and lamb ($r_{cv} = 0.69$) were determined reasonably.

Accurate meat classification is important for its pricing, authentication, and grouping to meet special requirements of consumers. Meat grading is commonly carried out by experienced human inspector according to grading standards or by some chemical techniques.

However, these methods with shortcomings of being time-consuming and destructive are not suitable for rapid inspection. Previous attempts on the classification of pork were carried out using the hyperspectral imaging technique within the wavelength range of about 400–1000 nm (Elmasry & Sun, 2010). However their classification rates were generally below 90%. Instead of considering the visible and short-wave near infrared spectral (about 400–1000 nm), the long-wave near infrared spectral with the wavelength range of 900–1700 nm was applied for grading pork cuts from three quality grades (PSE, RFN and DFD) (Barbin, Elmasry, Sun, & Allen, 2012a). On the basis of selected spectra of lonely loin eye area, they executed spectral preprocessing and wavelength selection, resulting in an overall accuracy of 96%, which is better than the results of previous works. Hyperspectral imaging was also found to be more efficient than computer vision and Minolta chromameter for the discrimination of three types of lamb muscles (Kamruzzaman, ElMasry, Sun, & Allen, 2011). The overall classification accuracy increased from 81.9% and 89.5% to 100%. In another study, the potentiality of NIR hyperspectral imaging as an objective and non-destructive method was investigated for the authentication and classification of cooked turkey ham slices (ElMasry, Iqbal, Sun, Allen, & Ward, 2011a). The linear discriminant analysis calibration model with effective wavelengths correctly classified 100% of all ham quality classes. The spectral data at only effective wavelengths were believed to contain ham quality class membership (ElMasry et al., 2011a). Cooling (Hu and Sun, 2000; Wang and Sun, 2001, 2002; Sun and Zheng, 2006; Sun and Hu, 2003) and freezing (Li and Sun, 2002) are commonly used methods for maintaining food quality, besides quality grades, hyperspectral imaging was also found to be effective in the discrimination of fresh and frozen-thawed pork in 900–1700 nm (Barbin, Sun, & Su, 2013), the authentication of different red meat species (Kamruzzaman, Barbin et al. 2012a), the quantification of adulteration in minced lamb meat (Kamruzzaman, Sun, ElMasry & Allen, 2013), classification of pig fat samples from different subcutaneous layers (Foca et al., 2013), and classification of Spanish cooked ham (Talens et al., 2013).

Currently, the quality parameters, which have been investigated for meat and meat products, mainly include tenderness which were measured as slice shear force (SSF) or WBSF, water content, WHC/drip loss, fat and fatty acids, contamination (fecal material or ingesta), microbial spoilage (TVC or other bacteria), tumor, bone fragments, color, pH, protein, grade classification and authentication (Table 1). Among them, tenderness, fat, color, and pH have been investigated in many works and good results were obtained for these attributes. As the near infrared region has rich information of water (O–H stretching third, second and first overtones around 760, 970, and 1440 nm, respectively), the assessments of water content and WHC also had good results. The studies on contamination, tumor and bone fragment detection were mainly focused on poultry, and were mostly based on several key wavelengths in order to increase the contrast between these substances to be detected and the background (poultry). Currently, the spoilage determination mainly focuses on TVC that is the total viable bacterial count. In the future, more specific bacterial for meat should be considered. Besides quality assessment and safety detection, classification of meat with different grades has also been investigated. Some works have also focused on fresh and frozen-thawed discrimination, authentication, and adulteration detection for some meats. More works should be conducted on classification, discrimination, authentication, and adulteration of meat and meat products in the future.

3. Quality and safety analysis and assessment of fish

Fish and fish products are of great dietary benefits for human health. Quality and safety inspection and documentation of fish and fish products through the whole value chain are extremely important for both consumers and producers. The first application of hyperspectral imaging for the quantitative measurement of fish quality was carried out in 2006 for moisture determination, and followed by determining fat distribution (Elmasry & Sun, 2010). Since 2010, more and more attributes of fish have been assessed by using hyperspectral imaging technology, including color (Wu, Sun, & He, 2012c), moisture (He, Wu, & Sun, 2013), texture (Wu, He, & Sun, 2012a), pH (He, Wu, & Sun, 2012), WHC (Wu & Sun 2013b) ice fraction (Stevik et al., 2010), astaxanthin (Dissing, Nielsen, Ersboll, & Frosch, 2011), and microbial spoilage (Wu & Sun, 2013a). Among these attributes, most of them were well predicted ($r > 0.8$) by analyzing hyperspectral images. It was noticed that except determining color, other attributes were measured using hyperspectral imaging systems within the wavelength ranges of visible and short-wave near infrared region (about from 400 nm to 1000 nm). This might be because the systems in this range are cheaper than those within long-wave near infrared region (900–1700 nm). As more information of hydrogen containing bonds is contained in long-wave near infrared region, this wavelength range should be considered in the future research for fish quality assessment. Another conclusion is that all of these researches used PLSR for multivariate data analysis, which is a classic linear calibration method. More efforts should be conducted on evaluating non-linear methods such as ANN and support vector regression (SVR). As we know, hyperspectral images contain redundant spectral information with a serious problem of multicollinearity among contiguous variables. However, the current works on determining fish quality attributes are only considered the model calibration based on full range spectra, except the works on color, moisture, WHC, and microbial spoilage determination. Therefore, optimal wavelength selection should be considered for assessing these attributes to minimize the multicollinearity and speed up the subsequent data processing. In the attempt of color determination and visualization made by Wu et al. (2012c), they proposed a novel idea of identifying instrumental effective wavelengths (IEW) for the prediction of all three color components instead of selecting different sets of effective wavelengths for each color component respectively, leading to reducing the number of band-pass filters for designing the multispectral imaging system. Meanwhile, predictive effective wavelengths (PEW) were further chosen from IEW to optimize calibration models. In addition, salmon was found to be the most preferred fish for assessing quality attributes using hyperspectral imaging, while there were many different kinds of fish considered in the fat and moisture determination. Therefore, other varieties of fish should be investigated for measurement of quality attributes in the future.

Candling and manual inspection are still used as the commercial way of quality inspection of fish, which are however inefficient, time-consuming, laborious, and costly. In this sense, hyperspectral imaging has been used for detecting fish ridge and nematodes in filets (Elmasry and Sun, 2010). Although many applications have used hyperspectral imaging systems in reflectance mode, transmission mode was more popular in detecting nematode (Elmasry and Sun, 2010; Sivertsen, Heia, Hindberg, & Godtliebsen, 2012; Sivertsen, Heia, Stormo, Elvevoll, & Nilsen, 2011a). Recently, a system capable of automatic detection of nematodes in full size cod filets was presented at a belt speed of 25 mm/s (Sivertsen et al., 2011a). The performance of the system was comparable to manual detection on candling tables. However, the system could not process the filets with skin and had a slow speed. A new hyperspectral imaging system for automatic detection of nematodes in cod filets was further developed, operating at a conveyor belt speed of 400 mm/s to meet the industrial required speed (Sivertsen et al., 2012). The improvements of the new system included using a fiber optic light line on both sides of the imaging area and adopting the interactance mode that can eliminate the effect of specular reflection, and increase the signal received from inside the sample (Sivertsen, Kimiya, & Heia, 2011b). As a result, the Gaussian maximum likelihood (GML) classifier detected 70.8% and 60.3% of the dark and pale nematodes, respectively, which is

Table 1
Summary of applications of hyperspectral imaging for evaluating quality attributes of meat and fish since 2010.

Quality attributes	Product	Imaging mode	Wavelength range (nm)	Multivariable analysis	Variable selection	Accuracy	References
Tenderness	Beef	Scattering	400–1100	MLR	Yes	$r_{cv} = 0.86$	Wu et al. (2010)
Tenderness	Beef	Scattering	400–1100	MLR	Yes	$r_{cv} = 0.91$	Wu et al. (2012d)
Tenderness	Pork	Scattering	400–1000	MLR	Yes	r = 0.831–0.930	Tao et al. (2012)
Tenderness	Beef	Reflectance	900–1700	PLSR	Yes	$r^2 = 0.83$	ElMasry et al. (2012)
Tenderness	Lamb	Reflectance	900–1700	PLSR, MLR, SPA	Yes	r = 0.84	Kamruzzaman et al.
Water	Lamb	Reflectance	900–1700	PLSR	Yes	r_p^2 of 0.88	Kamruzzaman et al. (2012b)
Water	Pork	Reflectance	900–1700	PLSR	Yes	r_p^2 of 0.87	Barbin et al. (2012b)
Water	Beef	Reflectance	900–1700	PLSR	Yes	r_p^2 of 0.89	ElMasry et al. (2013)
Water	Turkey hams	Reflectance	900–1700	PLSR	Yes	r_{cv}^2 of 0.88	Iqbal et al. (2013)
Water	Cooked ham	Reflectance	900–1700	PLSR	Yes	r_{cv}^2 of 0.868	Talens et al. (2013)
WHC	Beef	Reflectance	910–1700	PCA & PLSR	Yes	r^2 = 0.87–0.89	ElMasry et al. (2011b)
WHC	Pork	Reflectance	900–1700	PLSR	Yes	$r^2 = 0.83$	Barbin et al. (2012c)
WHC	Lamb	Reflectance	900–1700	PLSR	Yes	$r^2 = 0.77$	Kamruzzaman et al. (2012c)
Fat	Beef	Interactance	760–1040	PLSR	No	r = 0.98	Wold et al. (2011)
Fat	Pork	Interactance	760–1040	PLSR	No	RMSEP of 1.3%–3.4%	O'Farrell et al. (2010)
Fat	Pork	Reflectance	900–1700	PLSR	Yes	r_{cv}^2 of 0.95	Barbin et al. (2012b)
Fat	Lamb	Reflectance	900–1700	PLSR	Yes	r_{cv}^2 of 0.91	Kamruzzaman et al. (2012b)
Fat	Beef	Reflectance	900–1700	PLSR	Yes	r_p^2 of 0.91	ElMasry et al. (2013)
Fat	Cooked ham	Reflectance	900–1700	PLSR	No	$r^2 = 0.369$	Talens et al. (2013)
Fat and fatty acids	Beef	Reflectance	1000–2300	PLSR	No	$r^2 = 0.90$ for total fat; $r^2 = 0.87$ for SEA; $r^2 = 0.89$ for UFA	Kobayashi et al. (2010)
Contamination	Poultry	Reflectance	400–1000	BR	Yes	89%–98%	Yoon et al. (2011)
Wholesome/ unwholesome	Poultry	Reflectance	389–744	BR	Yes	over 95%	Chao et al. (2010); Yang et al. (2010)
Microbial spoilage	Pork	Reflectance	400–1000	MLR, PLSR, ANN, & LS-SVM	No	$r^2 = 0.9872$	Tao et al. (2010); Wang et al. (2010b); Wang et al. (2011c)
TVC	Chicken filet	Reflectance	900–1700	PLSR	Yes	r = 0.94–0.96	Feng and Sun, 2012
Pseudomonas	Chicken filet	Reflectance	900–1700	PLSR, GA	Yes	r = 0.87–0.91	Feng and Sun (2013)
Enterobacteriaceae	Chicken filet	Reflectance	900–1700	PLSR	Yes	r^2 = 0.86–0.89	Feng et al. (2012)
TVC and PPC	Porcine meat	Reflectance	900–1700	PLSR	Yes	$r^2 = 0.86$ for TVC; $r^2 = 0.89$ for PPC	Barbin et al. (2012d)
Microbial spoilage	Beef	Scattering	400–1000	MLR	Yes	$r^2 = 0.95$	Peng et al. (2011)
Microbial spoilage	Pork	Scattering	400–1000	MLR	Yes	r = 0.841–0.877	Tao et al. (2012)
Color and pH	Beef	Reflectance	900–1700	PLSR	Yes	$r_{cv}^2 = 0.88$ for L^*; $r_{cv}^2 = 0.80$ for b^*; $r_{cv}^2 = 0.71$ for pH	ElMasry et al. (2012)
Color and pH	Pork	Reflectance	900–1700	PLSR	Yes	$r_{cv}^2 = 0.87$ for pH; $r_{cv}^2 = 0.93$ for L^*; $r_{cv}^2 = 0.75$ for a^*; $r_{cv}^2 = 0.89$ for b^*; $r_{cv}^2 = 0.83$ for Chroma; $r_{cv}^2 = 0.81$ for Hue angle	Barbin et al. (2012c)
Color and pH	Lamb	Reflectance	900–1700	PLSR	Yes	$r_{cv}^2 = 0.65$ for pH; $r_{cv}^2 = 0.91$ for L^*	Kamruzzaman et al. (2012c)
Color and pH	Turkey hams	Reflectance	900–1700	PLSR	Yes	$r_{cv}^2 = 0.81$ for pH; $r_{cv}^2 = 0.18$ for L^*; $r_{cv}^2 = 0.72$ for a^*; $r_{cv}^2 = 0.49$ for b^*	Iqbal et al. (2013)
Color and pH	Beef	Scattering	400–1100	MLR	Yes	$r_{cv} = 0.96$ for L^*; $r_{cv} = 0.96$ for a^*; $r_{cv} = 0.97$ for b^*	Wu et al. (2010)
Color and pH	Beef	Scattering	400–1100	MLR	Yes	$r_{cv} = 0.92$ for L^*; $r_{cv} = 0.90$ for a^*; $r_{cv} = 0.88$ for b^*	Wu et al. (2012d)
Protein	Lamb	Reflectance	900–1700	PLSR	Yes	r_{cv}^2 of 0.85	Kamruzzaman et al. (2012b)
Protein	Pork	Reflectance	900–1700	PLSR	Yes	r_{cv}^2 of 0.91	Barbin et al. (2012b)
Protein	Beef	Reflectance	900–1700	PLSR	Yes	r_p^2 of 0.91	ElMasry et al. (2013)
Protein	Spanish cooked ham	Reflectance	900–1700	PLSR	Yes	$r_{cv}^2 = 0.855$	Talens et al. (2013)
Sensory	Lamb	Reflectance	900–1700	PLSR	Yes	$r_{cv} = 0.69$ for tenderness	Kamruzzaman et al.
Sensory	Pork	Reflectance	900–1700	PLSR	Yes	$r_{cv}^2 = 0.49$ for juiciness; $r_{cv}^2 = 0.54$ for tenderness	Barbin et al. (2012c)
Grade	Pork	Reflectance	900–1700	PCA	Yes	96%	Barbin et al. (2012a)
Grade	Lamb	Reflectance	900–1700	PCA & LDA	Yes	100%	Kamruzzaman et al. (2011)
Grade	Ham	Reflectance	900–1700	PCA & LDA	Yes	100%	ElMasry et al. (2011a)
Fresh and frozen-thawed	Pork	Reflectance	900–1700	PLS-DA	Yes	100%	Barbin et al. (2013)
Authentication	Lamb	Reflectance	900–1700	PCA, PLS-DA	Yes	98.67%	Kamruzzaman, Barbin et al. (2012a)
Adulteration	Lamb	Reflectance	900–1700	PCA, PLSR, MLR	Yes	$r_{cv}^2 = 0.98$	Kamruzzaman, Sun et al. (2013)
Classification		Reflectance	960–1700	PCA, PLS-DA, WPTER	Yes	96%	Foca et al. (2013)

(continued on next page)

Table 1 (*continued*)

Quality attributes	Product	Imaging mode	Wavelength range (nm)	Multivariable analysis	Variable selection	Accuracy	References
	Pig subcutaneous layers						
Classification	Cooked ham	Reflectance	900–1700	PLS-DA	Yes	$r^2_{cv} = 0.952$	Talens et al. (2013)
Color	Salmon	Reflectance	900–1700	PCA, PLSR, MLR, SPA,	Yes	r = 0.876 for L^*; r = 0.744 for a^*; r = 0.803 for b^*	Wu et al. (2012c)
Texture	Salmon	Reflectance	400–1000	PLSR	No	r = 0.66 for hardness; r = 0.56 for cohesiveness; r = 0.61 for adhesiveness	Wu et al. (2012a)
Moisture	Salmon	Reflectance	400–1000 & 900–1700	PLSR	Yes	$r^2 = 0.884–0.893$	He et al. (2013)
WHC	Salmon	Reflectance	400–1000 & 900–1700	PLSR, LS-SVM, CARS	Yes	$r_p = 0.815–0.970$	Wu & Sun, 2013b
pH	Salmon	Reflectance	400–1000	PLSR	No	r = 0.894	He et al. (2012)
Ice fraction	Salmon	Interactance	760–1040	PLSR	No	r = 0.9–0.96	Stevik et al. (2010)
Astaxanthin	Rainbow trout	Reflectance	385–970	PCA & PLSR	No	$r^2 = 0.86$	Dissing et al. (2011)
TVC	Salmon	Reflectance	400–1700	PLSR, LS-SVM, CARS	Yes	$r^2_p = 0.985$	Wu et al. (2013)
Nematodes	Cod	Transmittance	400–1000	FDR	No	58%	Sivertsen et al. (2011a)
Nematodes	Cod	Interactance	400–1000	GML		70.8% (dark nematodes); 60.3% (pale nematodes)	Sivertsen et al. (2012)
Frozen-thawed	Cod	Interactance	400–1000	PCA, Knn, PLSR	Yes	r = 0.82–0.93	Sivertsen et al. (2011b)
Frozen-thawed	Halibut	Reflectance	380–1030	PCA, GLCM, LS-SVM	No	97.22%	Zhu et al. (2013a)
Expired	Salmon	Reflectance	400–1000	PLS-DA	No	82.7%	Ivorra et al. (2013)
Classification	Sea bass	Reflectance	400–970	PLSR	No	87% (48 h post-mortem); 67% (96 h post-mortem)	Costa et al. (2011)
Classification	Salmon	Interactance	400–1000	PCA, PLSR	Yes	>88%	Sone et al. (2012)

Abbreviations: r: Correlation Coefficient, r^2: Coefficient of Determination, r_{cv}: Correlation Coefficient for Cross Validation, r^2_{cv}: Coefficient of Determination for Cross Validation, r^2_p: Coefficient of Determination for Prediction, MLR: Multi-Linear Regression, PLSR: Partial Least Squares Regression, SPA: Successive Projections Algorithm, PCA: Principal Component Analysis, BR: Band Ratio, ANN: Artificial Neural Networks, LS-SVM: Least Squares Support Vector Machine, GA: Genetic Algorithm, LDA: Linear Discriminant Analysis, PLS-DA: Partial Least Squares Discriminant Analyses, WPTER: Wavelet Packet Transform for Efficient pattern Recognition, CARS: Competitive Adaptive Reweighted Sampling, FDR: Fisher Discriminant Ratio, GML: Gaussian maximum likelihood.

better than the previous work (Sivertsen et al., 2011a) using a higher resolution instrument on a slow moving conveyor belt, and comparable or better to what is reported for manual inspection under industrial conditions (Sivertsen et al., 2012).

The determination of fish freshness is important for improving the ability to market fish on value and inspecting and managing the freshness of fish in the supply chain to reduce waste. Previous studies showed that it is feasible of using hyperspectral imaging for freshness identification (Elmasry and Sun, 2010; Menesatti, Costa, & Aguzzi, 2010). Recently, an imaging spectrometer system with interactance mode was developed for conducting online analysis of the freshness as a function of days-on-ice at an industrial speed of one filet per second or 40 cm/s Sivertsen et al. (2011b). Results show that freshness as days on ice can be determined with r = 0.82–0.91 on individual filets using the imaging system. In another study, fresh, fast frozen-thawed, and slow frozen-thawed fish filets were successfully distinguished with average correct classification rate of 97.22% based on both spectral and textural features extracted from hyperspectral images (Zhu, Zhang, He, Liu, & Sun, in press). Hyperspectral imaging was also used for detection of expired vacuum-packed smoked salmon with a classification success rate of 82.7% (Ivorra et al., 2013). Besides freshness identification, hyperspectral imaging also showed good abilities for discriminating concrete tank-cultured sea bass from sea cage-cultured sea bass at 48 and 96 h post-mortem Costa et al. (2011) and classifying Atlantic salmon (*Salmo salar* L.) filets stored under different atmospheres (Sone, Olsen, Sivertsen, Eilertsen, & Heia, 2012). However, compared with spectroscopy, applications of hyperspectral imaging in the freshness grading and quality classification have a limited number of publications, especially only focusing in a few varieties of fish. Therefore, the full potential of hyperspectral imaging on grading and classification should be exploited in the future works.

4. Quality and safety analysis and assessment of fruit and vegetables

Consumers would like to pay more for prime fruit and vegetables with superior quality and safety guaranteed. Hyperspectral imaging has been proved its great capability for the quality and safety assessment of fruit and vegetables, such as contamination, bruises, surface defects, starch index, firmness, SSC, sugar content, bitter pit, and chilling injury/freeze damage (Lorente et al., 2012; Nicolai et al., 2007; Sun, 2010).

The presence of defects is an important quality factor to influence the quality and price of fresh fruit and vegetables. Hyperspectral imaging has been used for detection of surface defects of apple, cherry, and citrus (Lorente et al., 2012; Nicolai et al., 2007) and internal defect of cucumber (Ariana & Lu, 2010a). Recently, more works have been conducted using hyperspectral imaging for the defect detection of not only previously analyzed fruits and vegetables like apple (Yang, Kim, & Chao, 2012c) and orange (Li, Rao, & Ying, 2011), but also other species, such as tomato (Cho et al., 2013) and onion (Wang et al., 2010a). These works were mainly conducted based on the scheme including the identification of spectral feature wavelengths of the defect(s) and using these spectral signatures to establish discrimination models.

As a main external defect, bruise damage is a main cause for the quality loss and degradation of fruit, which usually occurs during the harvest or transport process. Apple is the main research object for the detection of bruise damage using hyperspectral imaging in the last decade (Lorente et al., 2012; Nicolai et al., 2007; Sun, 2010). Besides apple, hyperspectral imaging has also been used for the bruise detection of pear (Zhao, Ouyang, Chen, & Wang, 2010) and kiwifruit (Lü, Tang, Cai, Zhao, & Vittayapadung, 2011). In recent years, various methods have been applied to selection of informative

wavelengths for online applications. Luo, Takahashi, Kyo, and Zhang (2012) considered each of the wavelength as an independent classifier and used receiver operating characteristic (ROC) analysis to select the best classifiers based on their performance. In order to develop a low-cost robust multispectral system for mushroom quality control, Esquerre, Gowen, Downey, and O'Donnell (2012) identified wavelengths with the most stable normalized regression coefficients using ensemble Monte Carlo variable selection (EMCVS). From the above researches, it was found that some of the wavelengths in the full-spectrum may be relevant to bruised or not, and would be important for the bruise detection. In another study, hyperspectral imaging (400–2500 nm) was incorporated with thermal imaging (3500–5000 nm) for detecting bruises created 1 h before the bruise assessments (Baranowski, Mazurek, Wozniak, & Majewska, 2012). The results showed that the joint application obtained best prediction efficiency for distinguishing bruised and sound tissues as well as bruises of various depths. In the future, more efforts should be made on the early detection of bruise damage before it is recognized by naked eyes.

Decay is another main defect of fruit affecting the post-harvest storage and transport. Hyperspectral imaging has been used for early automatic detection of fungal infections in post-harvest citrus fruits, instead of the manual detection carried out by trained workers illuminating the fruit with dangerous ultraviolet lighting. Recently, more attention has been made to select spectral features from hyperspectral images. Lorente, Aleixos, Gómez-Sanchis, Cubero, and Blasco (2013) proposed a methodology of ROC curve to select optimal features for decay detection in citrus fruit caused by two different fungi; *Penicillium digitatum* and *Penicillium italicum*. There were 74 features considered, including 57 purely spectral variables and 17 spectral indexes. The ROC method was found to be better than other common feature selection methods in most cases (Lorente, Blasco et al., 2013b).

Citrus canker is a serious disease affecting most commercial citrus species that is caused by the bacterium *Xanthomonas axonopodis*. In recent years, more efforts were made on selecting critical bands of the hyperspectral image data for developing multispectral methods to inspect citrus canker. The two-band ratio ($R_{834\ nm}/R_{729\ nm}$) selected by correlation analysis (CA) gave the maximum absolute correlation value of 0.811 in the correlation analysis. Two-band ratio images based on these two wavelengths had the classification accuracies in the range of 93.3–96.7% for each month (Zhao, Burks, Qin, & Ritenour, 2010b). Fig. 2 shows band ratio images of a cankerous grapefruit based on wavelengths selected by CA and PCA. Two-band ratio ($R_{834\ nm}/R_{729\ nm}$) outperformed the PCA-selected bands ($R_{907\ nm}/R_{718\ nm}$) in terms of classification performance owing to its supervised nature (Qin, Burks, Zhao, Niphadkar, & Ritenour, 2011). On the basis of the identified two important bands, a one-line commercial fruit sorting machine was developed with a speed of 5 fruits/s, and achieved an overall classification accuracy of 95.3% (Qin, Burks, Zhao, Niphadkar, & Ritenour, 2012).

Detection of fecal contamination on fruit and vegetables is important as feces are the source of a quantity of pathogens. Many works suggested that hyperspectral fluorescence imaging has better capability of determining the trace fecal spots than hyperspectral reflectance imaging, although the cost and stability of the excitation laser for fluorescence detection remain a question for practical implementation (Liu, Chen, Kim, Chan, & Lefcourt, 2007). Recently, violet 410-nm light-emitting-diode (LED) line lights were selected to provide near-uniform illumination to the linear field of view in a low cost way (Yang et al., 2011). Besides LEDs, the hyperspectral line-scan imaging system that Yang et al. (2011) developed also assembled an electron multiplying charge coupled device (EMCCD) camera, which was capable of acquiring high-resolution images at high speed under low illumination environments. The algorithms that utilized the fluorescence intensities at four wavebands (680, 684, 720, and 780 nm) detected more than 99% of the fecal spots (Yang et al., 2012a). Utilizing the same system, Yang, Kim, Millner, Chao, and Chan (2012b) proposed an algorithm based on the fluorescence intensities at two wavebands, 664 nm and 690 nm, for computation of the simple ratio function for effective detection of frass contamination on mature tomatoes.

Detection of insect damages in fruit and vegetables is another challenge as they can cause serious economic loss. Hyperspectral imaging has been applied to detect not only external insect infections such as in jujube fruit (Wang, Nakano et al., 2011b), mango (Saranwong et al., 2011), cucumber (Lu & Ariana, 2013), and mung bean (Kaliramesh et al., 2013), but also internal infections such as in vegetable soybeans (Huang, Wan, Zhang, & Zhu, 2012). All of the above works selected about 400–1000 nm to be the spectral range for the acquisition of hyperspectral images, except the work on jujube fruit that acquired the images mainly within the visible range (400–720 nm) and the work on mung bean (1000–1600 nm). Reflectance mode was used in the jujube fruit and mung bean analyses and transmittance mode in the work on vegetable soybeans. For the work on cucumbers, both reflectance (450–740 nm) and transmittance (740–1000 nm) modes were integrated into one system for the image acquisition. Classification models were established for detection of insect damages in these works using algorithms such as linear

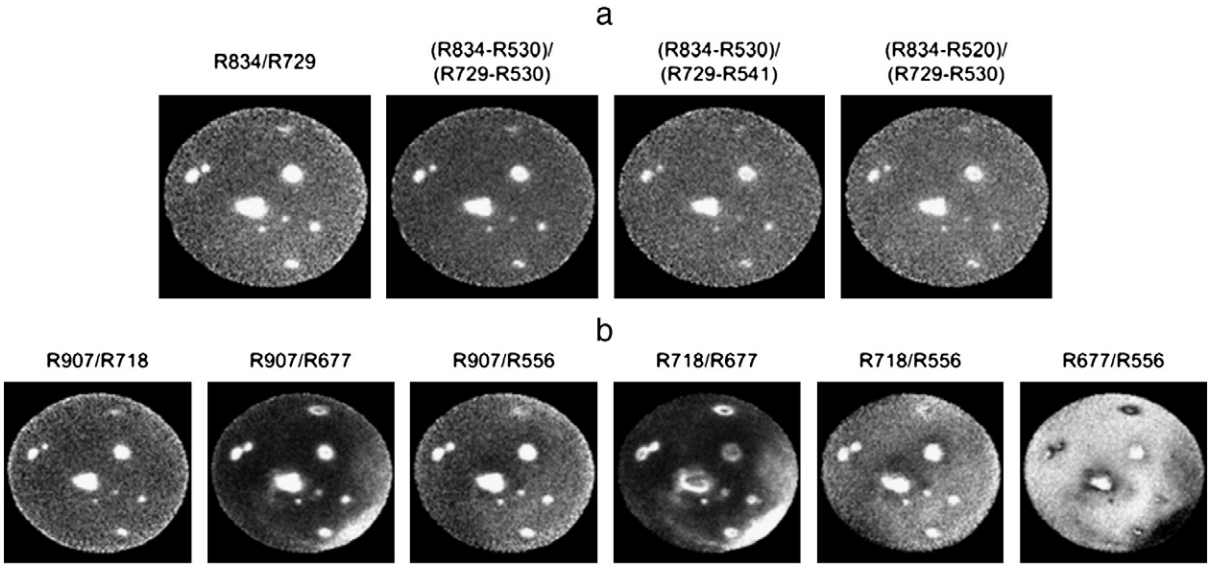

Fig. 2. Band ratio images of a cankerous grapefruit calculated using wavelengths selected from (a) correlation analysis and (b) principal components analysis (Qin et al., 2011).

discriminant analysis (LDA), quadratic discriminant analysis (QDA), stepwise discriminant analysis (SDA), iterative Bayesian discriminant analysis, partial least squares discriminant analyses (PLS-DA), and support vector data description (SVDD) classifier. Hyperspectral imaging technique showed better detection ability than manual inspection in the cucumber analysis (the overall actuaries of 82–93% vs. 75%), and also had good detection results for jujube (overall classification accuracy of 97.0%), mango (0.9% false negatives for infested fruit misclassified and 5.7% false positives for control fruit misclassified), mung bean (82–85%), and vegetable soybeans (95.6% overall classification accuracy).

Mealiness is a negative texture attribute that has the characteristics of abnormal softness tissues with lack of juiciness in the fruit. A series of works have been conducted on detecting mealiness in apple using hyperspectral imaging (Huang & Lu, 2010a; Huang & Zhu, 2011; Huang, Zhu, Wang, & Lu, 2012; Wang, Huang, Zhu, & Wang, 2011). All of these works acquired the hyperspectral images with the scatter mode in the spectral range of 600–1000 nm. PLS-DA and support vector machine (SVM) were two algorithms generally used in these works for the model calibration. Several feature selection methods, such as locally linear embedding (LLE) algorithm, uninformative variable elimination (UVE) coupled with LLE, and singular value decomposition (SVD) were applied for extracting features directly from hyperspectral images. In general, hyperspectral imaging had good two-class ('mealy' versus 'nonmealy') classification (about 75–85%), but did not give good results for three-class problem.

Surface color and moisture content are also important for evaluating the quality of fruit and vegetables. The current color measurements were mostly achieved by acquiring the hyperspectral images with reflectance mode in the range between 400 and 1000 nm, as it includes the visible spectral range (Ariana & Lu, 2010b; Taghizadeh, Gowen, & O'Donnell, 2011). The prediction of color was carried out in two ways, using tristimulus values calculated based on the hyperspectral images (Ariana & Lu, 2010b) and using multivariate algorithms such as PLSR (Taghizadeh et al., 2011). Hyperspectral imaging was found to have the similar ability for color determination compared with the colorimeter (Ariana & Lu, 2010b), and was believed to have more information of surface than RGB imaging (Taghizadeh et al., 2011). On the other hand, hyperspectral imaging with reflectance mode in the range between 400 and 1000 nm has been used for predicting moisture content of banana (Rajkumar, Wang, Eimasry, Raghavan, & Gariepy, 2012). Optimal wavelengths were selected for predicting moisture content using an exhaustive search with b-coefficients from PLSR models, resulting in coefficient of determination of 0.87.

Firmness and soluble solid content (SSC) are another two important quality attributes commonly used to determine maturity and harvest time of fruit and vegetables. A lot of endeavors have been made using hyperspectral imaging for the determination of firmness of fruits and vegetables, including apple, banana, strawberries, blueberries, pear, and peach (Cen, Lu, Mendoze, & Ariana, 2012; Leiva-Valenzuela, Lu, & Aguilera, 2012; Lorente et al., 2012; Nicolai et al., 2007). Most works used the hyperspectral or multispectral imaging systems with the scatter mode for firmness determination. Similar to firmness, the assessment of SSC was also conducted mostly using the hyperspectral imaging systems with the scatter mode for fruits such as apple, kiwifruit, melon, banana, strawberries, blueberries, pear, and grapes (Baiano, Terracone, Peri, & Romaniello, 2012; Cen et al., 2012; Leiva-Valenzuela et al., 2012; Lorente et al., 2012; Nicolai et al., 2007). Recently, more efforts have been made in the area of feature extraction, optimal wavelength selection, and data fusion with other techniques. Instead of using only the mean reflectance extracted from the hyperspectral scattering profiles, critical spectral and image features were extracted using spectral scattering profile and image analysis techniques, and then were integrated for predicting firmness and SSC of apples using PLSR method, outputting the SEP decrements of 6.6–13.7% and 3.0–11.2% for firmness and SSC, respectively (Mendoza, Lu, Ariana, Cen, & Bailey, 2011). On the other hand, some new algorithms were applied to select optimal wavelengths in the determination of firmness and SSC of fruit and vegetables, such as semi-supervised affinity propagation (AP) (NSAP) algorithm (Zhu, Huang, Zhao, & Wang, 2013), hierarchical evolutionary algorithm (HEA) coupled with subspace decomposition (Huang & Lu, 2010b), UVE and supervised affinity propagation (SAP) (Wang, Huang, & Zhu, 2012). From these works, it showed that the established models based on the wavelength selection yielded better results than the full spectrum models. In addition, considering that visible/near-infrared spectroscopy and hyperspectral scattering imaging have different sensing principles and have shown different abilities for predicting firmness and SSC, data fusion was conducted based on two technique to improve the prediction accuracy. It was found that VNIR spectroscopy had better ability in predicting SSC, while hyperspectral scattering imaging was superior for firmness prediction, and the data fusion of the two sensors produced significant improvements ($p < 0.05$) for prediction of the firmness and SSC than individual sensors (Mendoza, Lu, & Cen, 2011b).

Maturity stage of fruit is important to determine the best harvest data and optimize the post-harvest treatment and environment. Multispectral/hyperspectral imaging has been applied to determine the levels of maturity of peach and tomato (Herrero-Langreo, Lunadei, Lleó, Diezma, & Ruiz-Altisent, 2011; Lorente et al., 2012). The definition of wavelength ratio was a key target for the maturity evaluation, resulting in several optical indexes related to maturity stage (Lleo, Roger, Herrero-Langreo, Diezma-Iglesias, & Barreiro, 2011). Recently, six optical indexes, including Ind_1, Ind_2, Ind_3, I_{AD}, rir, and Icarot, were calculated from the data measured by multispectral imaging and spectrophotometer for the measurement of maturity in peach (Herrero-Langreo, Fernández-Ahumada, Roger, Palagós, & Lleó, 2012). The work on extracting mean reflectance spectra of grape seed in the range of 914–1715 nm to establish PLSR models showed a good prediction of maturation stage of grape seed with r^2 being higher than 0.95 (Rodríguez-Pulido et al., 2013).

5. Quality and safety analysis and assessment of grain

Hyperspectral imaging has also provided the light of success in the quality and safety assessment of the seeds of grain crops. There are many works which have been conducted for grain analysis using hyperspectral imaging since 1998, such as color classification of grain, vitreousness determination of wheat kernel, identification of sound or stained grains, classification of vitreous and non-vitreous wheat kernels, and discrimination of wheat classes (Jayas, Singh, & Paliwal, 2010). Recently, hyperspectral imaging in 700–1000 nm was combined with color imaging to identify wheat kernels damaged by some main insect damages (Singh, Jayas, Paliwal, & White, 2010b) and detection of midge-damaged wheat kernels (Singh, Jayas, Paliwal, & White, 2010a). In these works, six image features and ten histogram features were extracted from the most significant wavelengths determined according to the PCA analysis on hyperspectral images, and were then used to develop statistical discriminant classifiers (linear, quadratic, and Mahalanobis) or a back propagation neural network (BPNN) classifier for classification. Later, three types of wheat kernels (vitreous, yellow berry and fusarium-damaged) were successfully classified using hyperspectral imaging in near infrared field (1000–1700 nm) in tandem with PCA and PLS-DA (Serranti, Cesare, & Bonifazi, 2012).

Toxigenic fungi grown in grain are toxic for humans and animals. Hyperspectral imaging systems in visible and short-wave near infrared region (400–1000 nm) or long-wave near infrared region (960–1662 nm and 1000–2498 nm) has been successfully applied to indirectly detect *Fusarium* damage in maize (Williams, Manley, Fox, & Geladi, 2010) and wheat (Shahin & Symons, 2011), and also to investigate the fungal development (Williams, Geladi, Britz, & Manley, 2012). Besides *Fusarium*, the damage of other toxigenic fungi, such as *Aspergillus flavus*, *Aspergillus parasiticus*, *Aspergillus niger* on maize (Del Fiore et al., 2010) and wheat (Singh, Jayas, Paliwal, &

White, 2012) has also been detected by analyzing the hyperspectral images in 400–1000 nm or the combination of hyperspectral images in 700–1100 nm and color images. The quantitative determination of mycotoxin contamination is another issue for the grain industry. Hyperspectral imaging has been evaluated for predicting milled maize fumonisin contamination produced by *Fusarium* spp. (Firrao et al., 2010), and estimating aflatoxin concentration in corn kernels inoculated with *A. flavus* spores (Yao et al., 2010). Some correlations ($r^2 = 0.44$ by the MLR model and $r^2 = 0.68$ by the ANN model for fumonisin analysis, and $r^2 = 0.72$ by the MLR model for aflatoxin analysis) were obtained. In another study, Shahin, Symons, and Hatcher (2013) quantified mildew damage in soft red winter wheat by analyzing two kinds of spectral data, namely the spectra in 400–950 nm measured by a hyperspectral imaging system and the spectra in 1000–2500 nm measured by a Fourier Transform (FT)-NIR Analyzer. It was concluded that the spectra in the visible and shortwave-near-infrared range were more effective (classification accuracy of 96% (± 1 level)) for the quantification than the spectra in the long-wave near infrared range.

6. Other applications

Besides the investigation of using hyperspectral imaging technique on the quality and safety analysis and assessment of meat, fish, fruits, and vegetables, and grain, there are many other food products whose quality parameters were successfully determined on the basis of hyperspectral imaging in recent years.

Hyperspectral imaging has been investigated to be used for inspecting egg quality. Lunadei, Ruiz-Garcia, Bodria, and Guidetti (2012) designed a charged coupled device camera endowed with 15 monochromatic filters (440–940 nm) to classify dirty eggs whose eggshell presented organic residuals and clean eggs (including those with natural stains). The proposed classification algorithm was able to correctly classify nearly 98% of the samples with a very low processing time (0.05 s), and also showed a good robustness for an external sample set with a similar percentage of 97%. In another study, Abdel-Nour and Ngadi (2011) applied hyperspectral transmittance imaging (900–1700 nm) to classify eggs into three types with different docosahexaenoic acid contents using K-means analysis, resulting in 100% classification accuracy. Besides, PLSR models were established, which had r of 0.94, 0.73 and 0.87 for the prediction of alpha-linolenic acid, eicosapentaenoic acid, and docosahexaenoic acid, respectively. Recently, Liu and Ngadi (in press) detected fertility and early embryo development of chicken eggs using near-infrared hyperspectral imaging, resulting in best classification results of 100% at day 0, 78.8% at day 1, 74.1% at day 2, 81.8% at day 3, and 84.1% at day 4.

Cooked potato is popular in Europe and in many other countries. Hyperspectral interactance imaging in tandem with PLSR method obtained good prediction results with r of 0.99 and 0.97 for fat and dry matter and reasonable results with r of 0.83 for acrylamide prediction (Pedreschi, Segtnan, & Knutsen, 2010). Another work showed the ability of hyperspectral imaging to predict the optimal cooking time of boiled potatoes with less than 10% relative error (Nguyen Do Trong, Tsuta, Nicolai, De Baerdemaeker, & Saeys, 2011).

In addition, there are other food products which have been investigated for inspecting their quality attributes using hyperspectral imaging, such as classification of internally damaged almond nuts (Nakariyakul & Casasent, 2011), determination of edible meat content in crabs (Wold, Kermit, & Woll, 2010), and parasite detection in shell-free cooked clam (Coelho, Soto, Torres, Sbarbaro, & Pezoa, 2013). In order to detect the internal materials in samples such as internally damaged almond nuts, internal edible meat content in crabs, and internal parasite in clam, hyperspectral imaging systems in transmission or interactance mode in near infrared region (700–1400 nm, 760–1040 nm, and 600–950 nm) were established in the above mentioned works. Different classification or prediction strategies were applied in these works, such as Gaussian kernel based SVM model established based on the ratio of the responses at two different spectral bands (850 nm/1210 nm and 1160 nm/1335 nm) (Nakariyakul and Casasent, 2010), a piece-wise regression strategy with PLSR calibration (Wold et al., 2010), and a designed detector based on a reduced number of hyperspectral bands (624.1, 760.4, and 888.6 nm) (Coelho et al., 2013). Good output results were obtained in these works, namely 91.2% classification rate for internally damaged almond nuts, the result with r of 0.96 for predicting edible meat content in crabs, and 85% detection accuracy for parasite in clam.

7. Process assessments

In addition to the assessment of quality and safety attributes in final food products, it is also needed for inspection of these attributes of food products during some processes to understand and monitor the changes of these attributes in both quantitative and spatial distribution ways. There are several researches on using hyperspectral imaging for the determination of lycopene, lutein, β-carotene, chlorophyll-a, and chlorophyll-b concentrations during the ripening of tomatoes, which is a complex process including the breakdown of chlorophyll and build-up of carotenes (Lorente et al., 2012). Recently, more applications have been carried out using hyperspectral imaging for process assessment of food products, such as the prediction of moisture content of prawns during dehydration process (Wu et al., 2012b), the quality monitoring of continuous frying of minced beef and diced turkey (Daugaard, Adler-Nissen, & Carstensen, 2010), and tracking diffusion of conditioning water in single wheat kernels over time (Manley, du Toit, & Geladi, 2011). In addition, a novel technique called time series hyperspectral imaging (TS-HSI) was applied to determine the change of water distribution within beef during dehydration (Wu et al., 2013). TS-HSI is useful to achieve a complete understanding of processes in a sample, in the cases where a heterogeneous sample changes with time (Wu et al., 2013). The generated distribution maps in their study clearly showed the change of moisture distribution within beef during dehydration (Fig. 3). It is preponderant that the TS-HSI technique can be implemented in wide scales of quality inspection of numerous food products during process without additional laborious chemical analysis.

8. Application summary and future trends

The above reviews of previous researches proved the capability of hyperspectral imaging for inspecting different quality and safety attributes of numerous food products rapidly and non-invasively. By

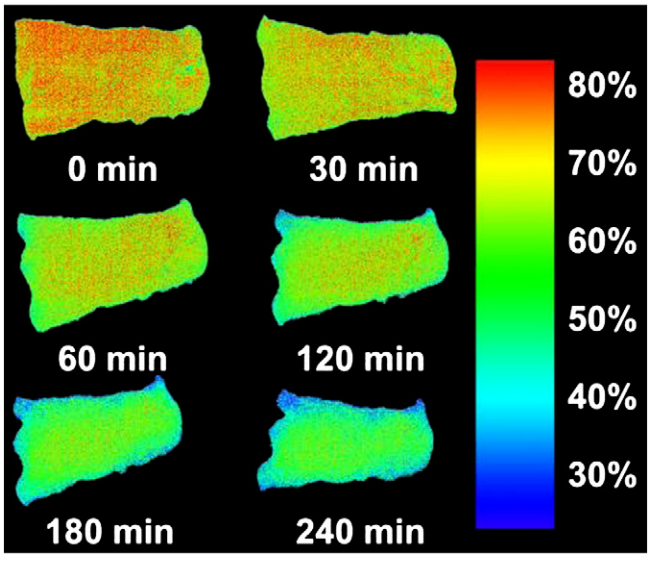

Fig. 3. Visualization of water distribution of beef slice during dehydration (Wu et al., 2013).

Table 2
Capabilities of hyperspectral imaging to inspect quality and safety attributes of fruits and vegetables since 2010.

Quality attributes	Product	Imaging mode	Wavelength range (nm)	Data analysis	Variable selection	Accuracy	References
Defect	Apple	Fluorescence	676, 714 and 779		Yes	Detected more than 95% of defect apples	Yang et al. (2012c)
Defect	Orange	Reflectance	400–1000	PCA, BR,	Yes	91.5% and 93.7% with no false positives	Li et al. (2011)
Defect	Tomato	Fluorescence	400–700	PCA	Yes	>99%	Cho et al. (2013)
Sour skin disease	Onion	Reflectance	950–1650	BPNN, SVM	Yes	80–100%	Wang et al. (2010a)
Bruise	Pear			PCA, MLC, EDC, MDC, SAM	No	93.8% by MDC; 95.0% by SAM	Zhao et al. (2010a)
Bruise	Kiwifruit	Reflectance	408–1117	SVM	Yes	12.5% error	Lü et al. (2011)
Bruise	Apple	Reflectance	380–1000	ROC, PLS-DA	Yes	Higher than 90%	Luo et al. (2012)
Bruise	Mushroom	Reflectance	880–1720	EMCVS, PLS-DA	Yes	100%	Esquerre et al. (2012)
Bruise	Apple	Reflectance	400–2500 3500–5000	PCA, MNF, SIMCA, LDA, SVM	No	95%	Baranowski et al. (2012)
Decay	Citrus	Reflectance	320–1020	ROC, MLP	Yes	89%	Lorente et al. (2013a)
Decay	Citrus	Reflectance	460–1020	ROC	Yes	87.46–95.52%	Lorente et al. (2013b)
Canker	Citrus	Reflectance	450–930	SID, BR	Yes	93.3–96.7%	Zhao et al. (2010b)
Canker	Citrus	Reflectance	450–930	CA, PCA	Yes	95.7%	Qin et al. (2011)
Canker	Citrus	Reflectance	730 and 830	BR	No	95.3%	Qin et al. (2012)
Contamination	Apple	Fluorescence	480–780	BR	Yes	96–100%	Yang et al. (2011)
Contamination	Apple	Fluorescence	480–780	BR	Yes	More than 99%	Yang et al. (2012a)
Contamination	Tomato	Fluorescence	664 and 690	BR	Yes	More than 99%	Yang et al. (2012b)
Insect damage	Jujube fruit	Reflectance	400–720	SDA	Yes	97.0%	Wang et al. (2011b)
Insect damage	Mango		400–1000	IBDA	No	0.9% false negatives for infested fruit misclassified and 5.7% false positives for control fruit misclassified	Saranwong et al. (2011)
Insect damage	Cucumber	Transmittance and reflectance	450–1000	PLS-DA	No	82–93%	Lu and Ariana (2013)
Insect damage	Mung bean	Reflectance	1000–1600	PCA, LDA, QDA	Yes	82–85%	Kaliramesh et al. (2013)
Insect damage	Vegetable soybean	Transmittance	400–1000	SVDD	No	95.6%	Huang et al. (2012a)
Mealiness	Apple	Scatter	600–1000	PLS-DA	No	74.6–86.7% for two classes 60.2–71.2% for three classes	Huang and Lu (2010a)
Mealiness	Apple	Scatter	600–1000	SVD & PLS-DA	No	76.1–80.6%	Huang and Zhu, (2011)
Mealiness	Apple	Scatter	600–1000	LLE, PLS-DA, SVM	No	80.4%, 82.5%	Huang et al. (2012b)
Mealiness	Apple	Scatter	600–1000	UVE, LLE, PLS-DA	No	74.9–79.8%	Wang et al. (2011a)
Color	Cucumber	Reflectance	400–1000	PCA	No	86%	Ariana and Lu (2010b)
Color	Mushroom	Reflectance	400–1000	PLSR	No	RMSECV = 1.5–2.8	Taghizadeh et al. (2011)
Moisture	Banana	Reflectance	400–1000	MLR, PLSR	Yes	r = 0.87	Rajkumar et al. (2012)
Firmness	Blueberry	Reflectance	500–1000	PLSR	No	r = 0.87	Leiva-Valenzuela et al. (2012)
Firmness	Peach	Scatter	515–1000	PLSR, LS-SVM	Yes	r = 0.749	Cen et al. (2012)
Firmness	Apple	Reflectance	500–1000	PLSR	Yes	r = 0.84–0.95	Mendoza et al. (2011)
Firmness	Apple	Scatter	500–1000	NSAP, PLSR	Yes	r = 0.862	Zhu, Zhang et al. (in press)
Firmness	Apple	Reflectance	680–980	HEA, PLSR	Yes	r = 0.857	Huang et al. (2012)
Firmness	Apple	Scatter	500–1000	UVE, SAP, PLSR	Yes	r = 0.828	Wang et al. (2012)
Firmness	Apple	Scatter	460–1100	PLSR, WT	No	r = 0.840–0.902	Mendoza et al. (2011)
SSC	Blueberry	Reflectance	500–1000	PLSR	No	r = 0.79	Leiva-Valenzuela et al. (2012)
SSC	Peach	Scatter	515–1000	PLSR, LS-SVM	Yes	r = 0.504	Cen et al. (2012)
SSC	Apple	Reflectance	500–1000	PLSR	Yes	r = 0.66–0.88	Mendoza et al. (2011)
SSC	Apple	Scatter	500–1000	NSAP, PLSR	Yes	r = 0.890	Zhu, Zhang et al. (in press)
SSC	Apple	Reflectance	680–980	HEA, PLSR	Yes	r = 0.822	Huang and Lu, (2010b)
SSC	Apple	Scatter	460–1100	PLSR, WT	No	r = 0.829–0.904	Mendoza et al. (2011b)
SSC	Grape	Reflectance	400–1000	PLSR	No	r^2 = 0.93–0.94	Baiano et al. (2012)
Maturity	Peach	Reflectance	680, 800	BR	Yes	70–80%	Herrero-Langreo et al. (2011)
Maturity	Peach	Reflectance	400–1000	BR	Yes	83%	Lleo et al. (2011)
Maturity	Grape seed	Reflectance	914–1715	PCA, DA, PLSR	Yes	r^2 higher than 0.95	Rodríguez-Pulido et al. (2013)

Abbreviations: r: Correlation Coefficient, r^2: Coefficient of Determination, PCA: Principal Component Analysis, BR: Band Ratio, BPNN: Back Propagation Neural Network, SVM: Support Vector Machine, MLC: Maximum Likelihood Classification, EDC: Euclidean Distance Classification, MDC: Mahalanobis Distance Classification, SAM: Spectral Angle Mapper, ROC: Receiver operating characteristic, PLS-DA: Partial Least Squares Discriminant Analyses, EMCVS: Ensemble Monte Carlo variable selection, MNF: Minimum Noise Fraction Transform, SIMCA: Soft Independent Modeling of Class Analogies, LDA: Linear Discriminant Analysis, MLP: Multilayer perceptron, SID: Spectral Information Divergence, CA: Correlation Analysis, SDA: Stepwise Discriminant Analysis, IBDA: Iterative Bayesian Discriminant Analysis, QDA: Quadratic Discriminant Analysis, SVDD: Support Vector Data Description Classifier, SVD: Singular Value Decomposition, LLE: Locally Linear Embedding, UVE: Uninformative Variable Elimination, DA: Discriminant Analysis, PLSR: Partial Least Squares Regression, MLR: Multi-Linear Regression, LS-SVM: Least Squares Support Vector Machine, NSAP: Semi-Supervised Affinity Propagation, HEA: Hierarchical Evolutionary Algorithm, SAP: Supervised Affinity Propagation, WT: Wavelet Transforms.

summarizing the state of the art of hyperspectral imaging for quality and safety evaluation of the main food products since 2010, some general conclusions were drawn from Tables 1 and 2.

Currently, hyperspectral imaging systems used mainly covered the visible and near infrared regions that are generally from 400 to 1700 nm. In specific, by using the detectors with different light sensitive materials, there are generally two wavelength ranges considered, 400–1000 nm and 900–1700 nm. The systems within 400–1000 nm were mainly used for fruit and vegetables, because they are generally cheaper than those within 900–1700 nm and are less influenced by water. On the other hand, as the values of meat and fish products are generally higher than fruit and vegetables, hyperspectral imaging in the range of 900–1700 nm has been investigated more for meat and fish products, and showed good prediction abilities than the range of 400–1000 nm in some cases. Due to their respective advantages and disadvantages, it is suggested that both the wavelength ranges of 400–1000 nm and 900–1700 nm should be considered and compared to find the best range. In addition, some cases have extended the wavelength region over 1700 nm, and some area detectors can even acquire the spectra in the mid-infrared region, which should be considered in the future research as the near infrared region having numerous overlapping bands without specific organic functional groups.

By studying the modes for acquisition of hyperspectral images, it was observed that reflectance was the most frequently used mode for either the meat and fish analysis (about 78% applications in Table 1) or the fruit and vegetable analysis (about 55% applications in Table 2). It might be because the reflectance mode can measure the spectra of surface and near surface parts of food products where many quality and safety attributes are related to, and is easy to be achieved for a hyperspectral imaging system with relatively low cost. Scattering mode is another commonly used mode, and showed better performances than reflectance mode in some cases. There were about 11% applications using scattering mode in Table 1 for inspecting attributes like tenderness, microbial spoilage, color and pH. In Table 2, there were about 23% applications which considered scattering mode for assessing attributes like mealiness, firmness, and SSC. Fluorescence mode is popularly used for defect and contamination detection of not only fruit and vegetables as shown in Table 2, but also for poultry carcass inspection (Chao, 2010; Elmasry & Sun, 2010). Transmittance mode is usually not used for food analysis, as food products are mostly opaque for light to transmit. A few applications considering transmittance mode included nematode detection in fish filet (Table 1) and insect damage detection of cucumber and soybean (Table 2). The interactance mode can detect deeper information into the sample, has less surface effects, and reduces the influence of thickness. In recent years, it has been used for fat assessment in meat and some applications of fish, such as nematode detection, ice fraction assessment, and freshness assessment (Table 1). It is noticed that for most researches only one mode was considered and only a few works used two modes. As each mode has its own advantages and disadvantages, it is suggested to investigate and compare different imaging modes in the future works.

Multivariate data analysis is an important step for processing massive spectral data of hyperspectral images. PLSR and PLS-DA are classical multivariate calibration algorithms for spectral calibration. About 76% applications in Table 1 and 51% applications in Table 2 used PLSR or PLS-DA as the calibration algorithm only or at least one of them for the purposes of regression or classification. MLR is another well-known method based on ordinary least squares regression. About 17% applications in Table 1 chose MLR for the spectral calibration. BR and BD were preferred in fruit and vegetable analysis (about 17% applications in Table 2), as they have very simple structures for the calibration model and are easily to be realized in inspection systems. Moreover, some non-linear regression techniques such as ANN and SVM would be suitable for the calibration. There are about 8% and 15% applications which considered ANN or SVM in Table 1 and Table 2, respectively. As it is not quite obvious whether there is more linear relationship or more non-linear relationship between the spectral data and target attributes, it is suggested to consider at least one linear and non-linear calibration methods in the hyperspectral image analysis. In addition, PCA is another commonly used method for the purpose of decreasing redundancy of hyperspectral images and generating score images to understand variations between different samples and within one sample. On the other hand, consideration of only informative variables instead of using all variables in the calibration process would make the calibrated model efficient and robust for predicting future samples. A number of variable selection algorithms have been applied in hyperspectral image analysis, such as ratio variable selection, regression coefficients from PLSR analysis, loading from PCA analysis, SPA, and GA. In order to select the most informative and effective variables with minimum number, it is suggested to consider different variable selection strategies and compare their performances to choose the best one. Visualization is an important and interested output of hyperspectral image analysis to show the detailed distribution of spatially non-homogeneous concentrates of attribute or the specific locations and shapes of defects or foreign matters in a food sample. However, the visualization is not all considered in previous researches, especially in the assessment of attribute concentrations. Therefore, besides quantitative prediction by establishing calibration models, visualization of attribute distribution should be also considered to understand the attribute variations of food products from sample to sample and even from position to position within the same sample.

Recent works show a bright future of using hyperspectral imaging for the quality inspection of more and more food products. The successful outcome of applying hyperspectral imaging would improve quality and safety measurement of finfish products to meet consumer expectations, label accurate quality factors on the packaging of retail products to benefit consumers, and help the food industry to better understand and control the food quality and safety, leading to increased competitiveness in international markets. However, there are still some limitations and restrictions to be overcome for hyperspectral imaging before moving this technology from the laboratories to the industry real-time inspections, including improving the hardware and software of hyperspectral imaging system to reduce the instrument cost and increase the measurement speed, extracting the most important object features from hyperspectral images to develop feature based imaging systems like multispectral imaging, investigating the most suitable model calibration strategy with high accuracy, efficiency, and robustness for the inspection, and transferring the systems and algorithms, which are dependent on the laboratory environment to industrial conditions.

9. Conclusions

Hyperspectral imaging is a complex, highly multidisciplinary field with the aim of realizing efficient and reliable measurement of both contents and spatial distributions of multiple chemical constituents and physical attributes simultaneously without monotonous sample preparation, and therefore offering the possibility of designing inspection systems for the automatic grading and nutrition determination of food products. The various applications outlined in this review show the capability of using hyperspectral imaging for sample classification and grading, defect and disease detection, distribution visualization of chemical attributes in chemical images, and evaluations of overall quality of meat, fruits, vegetables, and other food products. Moreover, currently some practical implementations for real-time monitoring are already available. It is anticipated that real-time food monitoring systems with this technique can be expected to meet the requirements of the modern industrial control and sorting systems in the near future.

Acknowledgments

The authors would like to acknowledge the financial support provided by the Irish Research Council for Science, Engineering and Technology under the Government of Ireland Postdoctoral Fellowship scheme.

References

Abdel-Nour, N., & Ngadi, M. (2011). Detection of omega-3 fatty acid in designer eggs using hyperspectral imaging. *International Journal of Food Sciences and Nutrition*, *62*(4), 418–422.

Ariana, D. P., & Lu, R. (2010a). Hyperspectral imaging for defect detection of pickling cucumbers. In D. -W. Sun (Ed.), *Hyperspectral imaging for food quality analysis and control* (pp. 431–448) (1st ed.). San Diego, California, USA: Academic Press/Elsevier.

Ariana, D. P., & Lu, R. F. (2010b). Evaluation of internal defect and surface color of whole pickles using hyperspectral imaging. *Journal of Food Engineering*, *96*(4), 583–590.

Baiano, A., Terracone, C., Peri, G., & Romaniello, R. (2012). Application of hyperspectral imaging for prediction of physico-chemical and sensory characteristics of table grapes. *Computers and Electronics in Agriculture*, *87*, 142–151.

Baranowski, P., Mazurek, W., Wozniak, J., & Majewska, U. (2012). Detection of early bruises in apples using hyperspectral data and thermal imaging. *Journal of Food Engineering*, *110*, 345–355.

Barbin, D. F., Elmasry, G., Sun, D. -W., & Allen, P. (2012a). Near-infrared hyperspectral imaging for grading and classification of pork. *Meat Science*, *90*(1), 259–268.

Barbin, D. F., ElMasry, G., Sun, D. -W., & Allen, P. (2012b). Non-destructive determination of chemical composition in intact and minced pork using near-infrared hyperspectral imaging. *Food Chemistry*, *138*(2–3), 1162–1171.

Barbin, D. F., ElMasry, G., Sun, D. -W., & Allen, P. (2012c). Predicting quality and sensory attributes of pork using near-infrared hyperspectral imaging. *Analytica Chimica Acta*, *719*(16), 30–42.

Barbin, D. F., ElMasry, G., Sun, D. -W., Allen, P., & Morsy, N. (2012d). Non-destructive assessment of microbial contamination in porcine meat using NIR hyperspectral imaging. *Innovative Food Science & Emerging Technologies*, *17*, 180–191.

Barbin, D. F., Sun, D. -W., & Su, C. (2013). NIR hyperspectral imaging as non-destructive evaluation tool for the recognition of fresh and frozen -thawed porcine longissimus dorsi muscles. *Innovative Food Science & Emerging Technologies*, *18*, 226–236.

Cen, H., Lu, R., Mendoze, F., & Ariana, D. (2012). Assessing multiple quality attributes of peaches using optical absorption and scattering properties. *Transactions of the ASABE*, *55*(2), 647–657.

Chao, K. (2010). Automated poultry carcass inspection by a hyperspectral–multispectral line-scan imaging system. In D. -W. Sun (Ed.), *Hyperspectral imaging for food quality analysis and control* (pp. 241–272) (1st ed.). San Diego, California, USA: Academic Press/Elsevier.

Chao, K. L., Yang, C. C., & Kim, M. S. (2010). Spectral line-scan imaging system for high-speed non-destructive wholesomeness inspection of broilers. *Trends in Food Science & Technology*, *21*(3), 129–137.

Cho, B. -K., Kim, M. S., Baek, I. -S., Kim, D. -Y., Lee, W. -H., Kim, J., et al. (2013). Detection of cuticle defects on cherry tomatoes using hyperspectral fluorescence imagery. *Postharvest Biology and Technology*, *76*, 40–49.

Coelho, P. A., Soto, M. E., Torres, S. N., Sbarbaro, D. G., & Pezoa, J. E. (2013). Hyperspectral transmittance imaging of the shell-free cooked clam Mulinia edulis for parasite detection. *Journal of Food Engineering*, *117*(3), 408–416.

Costa, C., D'Andrea, S., Russo, R., Antonucci, F., Pallottino, F., & Menesatti, P. (2011). Application of non-invasive techniques to differentiate sea bass (*Dicentrarchus labrax*, L. 1758) quality cultured under different conditions. *Aquaculture International*, *19*(4), 765–778.

Daugaard, S. B., Adler-Nissen, J., & Carstensen, J. M. (2010). New vision technology for multidimensional quality monitoring of continuous frying of meat. *Food Control*, *21*(5), 626–632.

Del Fiore, A., Reverberi, M., Ricelli, A., Pinzari, F., Serranti, S., Fabbri, A. A., et al. (2010). Early detection of toxigenic fungi on maize by hyperspectral imaging analysis. *International Journal of Food Microbiology*, *144*(1), 64–71.

Delgado, A. E., & Sun, D. -W. (2002). Desorption isotherms for cooked and cured beef and pork. *Journal of Food Engineering*, *51*(2), 163–170. http://dx.doi.org/10.1016/S0260-8774(01)00053-X.

Dissing, B. S., Nielsen, M. E., Ersboll, B. K., & Frosch, S. (2011). Multispectral imaging for determination of astaxanthin concentration in salmonids. *PLoS One*, *6*(5), e19032.

Du, C. J., & Sun, D. -W. (2005). Comparison of three methods for classification of pizza topping using different colour space transformations. *Journal of Food Engineering*, *68*(3), 277–287. http://dx.doi.org/10.1016/j.jfoodeng.2004.05.044.

ElMasry, G., Iqbal, A., Sun, D. -W., Allen, P., & Ward, P. (2011a). Quality classification of cooked, sliced turkey hams using NIR hyperspectral imaging system. *Journal of Food Engineering*, *103*(3), 333–344.

Elmasry, G., & Sun, D. -W. (2010). Meat quality assessment using a hyperspectral imaging system. In D. -W. Sun (Ed.), *Hyperspectral imaging for food quality analysis and control* (pp. 175–240) (1st ed.). San Diego, California, USA: Academic Press/Elsevier.

ElMasry, G., Sun, D. -W., & Allen, P. (2011b). Non-destructive determination of water-holding capacity in fresh beef by using NIR hyperspectral imaging. *Food Research International*, *44*(9), 2624–2633.

ElMasry, G., Sun, D. -W., & Allen, P. (2012). Near-infrared hyperspectral imaging for predicting colour, pH and tenderness of fresh beef. *Journal of Food Engineering*, *110*(1), 127–140.

ElMasry, G., Sun, D. -W., & Allen, P. (2013). Chemical-free assessment and mapping of major constituents in beef using hyperspectral imaging. *Journal of Food Engineering*, *117*(2), 235–246.

Esquerre, C., Gowen, A., Downey, G., & O'Donnell, C. (2012). Wavelength selection for development of a near infrared imaging system for early detection of bruise damage in mushrooms (*Agaricus bisporus*). *Journal of Near Infrared Spectroscopy*, *20*, 537.

Feng, Y. -Z., ElMasry, G., Sun, D. -W., Walsh, D., & Morcy, N. (2012). Near-infrared hyperspectral imaging and partial least squares regression for rapid and reagentless determination of Enterobacteriaceae on chicken fillets. *Food Chemistry*, *138*(2–3), 1829–1836.

Feng, Y. -Z., & Sun, D. -W. (2012). Determination of total viable count (TVC) in chicken breast fillets by near-infrared hyperspectral imaging and spectroscopic transforms. *Talanta*, *105*, 244–249.

Feng, Y. -Z., & Sun, D. -W. (2013). Near-infrared hyperspectral imaging in tandem with partial least squares regression and genetic algorithm for non-destructive determination and visualization of Pseudomonas loads in chicken fillets. *Talanta*, *109*, 74–83.

Firrao, G., Torelli, E., Gobbi, E., Raranciuc, S., Bianchi, G., & Locci, R. (2010). Prediction of milled maize fumonisin contamination by multispectral image analysis. *Journal of Cereal Science*, *52*(2), 327–330.

Foca, G., Salvo, D., Cino, A., Ferrari, C., Lo Fiego, D. P., Minelli, G., & Ulrici, A. (2013). Classification of pig fat samples from different subcutaneous layers by means of fast and non-destructive analytical techniques. *Food Research International*, *52*(1), 185–197.

Gowen, A. A., O'Donnell, C. P., Cullen, P. J., Downey, G., & Frias, J. M. (2007). Hyperspectral imaging — An emerging process analytical tool for food quality and safety control. *Trends in Food Science & Technology*, *18*(12), 590–598.

He, H. -J., Wu, D., & Sun, D. -W. (2012). Application of hyperspectral imaging technique for non-destructive pH prediction in salmon fillets. *Proceedings of the 3rd CIGR International Conference of Agricultural Engineering (CIGR-AgEng2012)* (Valencia, Spain).

He, H. -J., Wu, D., & Sun, D. -W. (2013). Non-destructive and rapid analysis of moisture distribution in farmed Atlantic salmon (Salmo salar) fillets using visible and near-infrared hyperspectral imaging. *Innovative Food Science & Emerging Technologies*, *18*, 237–245.

Herrero-Langreo, A., Fernández-Ahumada, E., Roger, J. M., Palagós, B., & Lleó, L. (2012). Combination of optical and non-destructive mechanical techniques for the measurement of maturity in peach. *Journal of Food Engineering*, *108*(1), 150–157.

Herrero-Langreo, A., Lunadei, L., Lleó, L., Diezma, B., & Ruiz-Altisent, M. (2011). Multispectral vision for monitoring peach ripeness. *Journal of Food Science*, *76*(2), E178–E187.

Hu, Z. H., & Sun, D. -W. (2000). CFD simulation of heat and moisture transfer for predicting cooling rate and weight loss of cooked ham during air-blast chilling process. *Journal of Food Engineering*, *46*(3), 189–197. http://dx.doi.org/10.1016/S0260-8774(00)00082-0.

Huang, M., & Lu, R. (2010a). Apple mealiness detection using hyperspectral scattering technique. *Postharvest Biology and Technology*, *58*(3), 168–175.

Huang, M., & Lu, R. (2010b). Optimal wavelength selection for hyperspectral scattering prediction of apple firmness and soluble solids content. *Transactions of the ASABE*, *53*(4), 1175–1182.

Huang, M., Wan, X., Zhang, M., & Zhu, Q. (2012a). Detection of insect-damaged vegetable soybeans using hyperspectral transmittance image. *Journal of Food Engineering*, *116*(1), 45–49.

Huang, M., & Zhu, Q. B. (2011). Feature extraction of hyperspectral scattering image for apple mealiness based on singular value decomposition. *Spectroscopy and Spectral Analysis*, *31*(3), 767–770.

Huang, M., Zhu, Q., Wang, B., & Lu, R. (2012b). Analysis of hyperspectral scattering images using locally linear embedding algorithm for apple mealiness classification. *Computers and Electronics in Agriculture*, *89*, 175–181.

Iqbal, A., Sun, D. -W., & Allen, P. (2013). Prediction of moisture, color and pH in cooked, pre-sliced turkey hams by NIR hyperspectral imaging system. *Journal of Food Engineering*, *117*(1), 42–51.

Ivorra, E., Girón, J., Sánchez, A. J., Verdú, S., Barat, J. M., & Grau, R. (2013). Detection of expired vacuum-packed smoked salmon based on PLS-DA method using hyperspectral images. *Journal of Food Engineering*, *117*(3), 342–349.

Jackman, P., Sun, D. -W., Du, C. -J., & Allen, P. (2008). Prediction of beef eating quality from colour, marbling and wavelet texture features. *Meat Science*, *80*(4), 1273–1281. http://dx.doi.org/10.1016/j.meatsci.2008.06.001.

Jayas, D. S., Singh, C. B., & Paliwal, J. (2010). Classification of wheat kernels using near-infrared reflectance hyperspectral imaging. In D. -W. Sun (Ed.), *Hyperspectral imaging for food quality analysis and control* (pp. 449–470) (1st ed.). San Diego, California, USA: Academic Press/Elsevier.

Kaliramesh, S., Chelladurai, V., Jayas, D., Alagusundaram, K., White, N., & Fields, P. (2013). Detection of infestation by *Callosobruchus maculatus* in mung bean using near-infrared hyperspectral imaging. *Journal of Stored Products Research*, *52*, 107–111.

Kamruzzaman, M., Barbin, D., ElMasry, G., Sun, D. -W., & Allen, P. (2012a). Potential of hyperspectral imaging and pattern recognition for categorization and authentication of red meat. *Innovative Food Science & Emerging Technologies*, *16*, 316–325.

Kamruzzaman, M., ElMasry, G., Sun, D. -W., & Allen, P. (2011). Application of NIR hyperspectral imaging for discrimination of lamb muscles. *Journal of Food Engineering*, *104*(3), 332–340.

Kamruzzaman, M., ElMasry, G., Sun, D. -W., & Allen, P. (2012b). Non-destructive prediction and visualization of chemical composition in lamb meat using NIR hyperspectral imaging and multivariate regression. *Innovative Food Science & Emerging Technologies*, *16*, 218–226.

Kamruzzaman, M., ElMasry, G., Sun, D. -W., & Allen, P. (2012c). Prediction of some quality attributes of lamb meat using near-infrared hyperspectral imaging and multivariate analysis. *Analytica Chimica Acta*, *714*, 57–67.

Kamruzzaman, M., ElMasry, G., Sun, D. -W., & Allen, P. (2013a). Non-destructive assessment of instrumental and sensory tenderness of lamb meat using NIR hyperspectral imaging. *Food Chemistry*, *141*(1), 389–396.

Kamruzzaman, M., Sun, D. -W., ElMasry, G., & Allen, P. (2013b). Fast detection and visualization of minced lamb meat adulteration using NIR hyperspectral imaging and multivariate image analysis. *Talanta*, *103*, 130–136.

Kobayashi, K., Matsui, Y., Maebuchi, Y., Toyota, T., & Nakauchi, S. (2010). Near infrared spectroscopy and hyperspectral imaging for prediction and visualisation of fat and fatty acid content in intact raw beef cuts. *Journal of Near Infrared Spectroscopy*, *18*(5), 301–315.

Leiva-Valenzuela, G. A., Lu, R., & Aguilera, J. M. (2012). Prediction of firmness and soluble solids content of blueberries using hyperspectral reflectance imaging. *Journal of Food Engineering*, *115*(1), 91–98.

Li, J. B., Rao, X. Q., & Ying, Y. B. (2011). Detection of common defects on oranges using hyperspectral reflectance imaging. *Computers and Electronics in Agriculture*, *78*(1), 38–48.

Li, B., & Sun, D. -W. (2002). Effect of power ultrasound on freezing rate during immersion freezing of potatoes. *Journal of Food Engineering*, *55*(3), 277–282. http://dx.doi.org/10.1016/S0260-8774(02)00102-4 (Article Number: PII S0260-8774(02)00102-4).

Liu, Y. L., Chen, Y. R., Kim, M. S., Chan, D. E., & Lefcourt, A. M. (2007). Development of simple algorithms for the detection of fecal contaminants on apples from visible/near infrared hyperspectral reflectance imaging. *Journal of Food Engineering*, *81*(2), 412–418.

Liu, L., & Ngadi, M. (2013). Detecting fertility and early embryo development of chicken eggs using near-infrared hyperspectral imaging. *Food and Bioprocess Technology*. http://dx.doi.org/10.1007/s11947-012-0933-3 (in press).

Lleo, L., Roger, J. M., Herrero-Langreo, A., Diezma-Iglesias, B., & Barreiro, P. (2011). Comparison of multispectral indexes extracted from hyperspectral images for the assessment of fruit ripening. *Journal of Food Engineering*, *104*(4), 612–620.

Lorente, D., Aleixos, N., Gómez-Sanchis, J., Cubero, S., & Blasco, J. (2013a). Selection of optimal wavelength features for decay detection in citrus fruit using the ROC curve and neural networks. *Food and Bioprocess Technology*, *6*, 530–541.

Lorente, D., Aleixos, N., Gomez-Sanchis, J., Cubero, S., Garcia-Navarrete, O. L., & Blasco, J. (2012). Recent advances and applications of hyperspectral imaging for fruit and vegetable quality assessment. *Food and Bioprocess Technology*, *5*(4), 1121–1142.

Lorente, D., Blasco, J., Serrano, A. J., Soria-Olivas, E., Aleixos, N., & Gómez-Sanchis, J. (2013b). Comparison of ROC feature selection method for the detection of decay in citrus fruit using hyperspectral images. *Food and Bioprocess Technology*. http://dx.doi.org/10.1007/s11947-012-0951-1 (in press).

Lu, R., & Ariana, D. P. (2013). Detection of fruit fly infestation in pickling cucumbers using a hyperspectral reflectance/transmittance imaging system. *Postharvest Biology and Technology*, *81*, 44–50.

Lü, Q., Tang, M. J., Cai, J. R., Zhao, J. W., & Vittayapadung, S. (2011). Vis/NIR hyperspectral imaging for detection of hidden bruises on kiwifruits. *Czech Journal of Food Sciences*, *29*(6), 595–602.

Lunadei, L., Ruiz-Garcia, L., Bodria, L., & Guidetti, R. (2012). Automatic identification of defects on eggshell through a multispectral vision system. *Food and Bioprocess Technology*, *5*, 3042–3050.

Luo, X., Takahashi, T., Kyo, K., & Zhang, S. (2012). Wavelength selection in vis/NIR spectra for detection of bruises on apples by ROC analysis. *Journal of Food Engineering*, *109*(3), 457–466.

Manley, M., du Toit, G., & Geladi, P. (2011). Tracking diffusion of conditioning water in single wheat kernels of different hardnesses by near infrared hyperspectral imaging. *Analytica Chimica Acta*, *686*(1–2), 64–75.

Mendoza, F., Lu, R., Ariana, D., Cen, H., & Bailey, B. (2011a). Integrated spectral and image analysis of hyperspectral scattering data for prediction of apple fruit firmness and soluble solids content. *Postharvest Biology and Technology*, *62*(2), 149–160.

Mendoza, F., Lu, R., & Cen, H. (2011b). Data fusion of visible/near-infrared spectroscopy and spectral scattering for apple quality assessment. *ASABE Annual International Meeting, Vol. 6.* (pp. 5084–5100) (Louisville, KY).

Menesatti, P., Costa, C., & Aguzzi, J. (2010). Quality evaluation of fish by hyperspectral Imaging. In D. -W. Sun (Ed.), *Hyperspectral imaging for food quality: Analysis and control* (pp. 273–294). San Diego, California, USA: Academic Press/Elsevier.

Nakariyakul, S., & Casasent, D. P. (2011). Classification of internally damaged almond nuts using hyperspectral imagery. *Journal of Food Engineering*, *103*(1), 62–67.

Nguyen Do Trong, N., Tsuta, M., Nicolai, B. M., De Baerdemaeker, J., & Saeys, W. (2011). Prediction of optimal cooking time for boiled potatoes by hyperspectral imaging. *Journal of Food Engineering*, *105*(4), 617–624.

Nicolai, B. M., Beullens, K., Bobelyn, E., Peirs, A., Saeys, W., Theron, K. I., et al. (2007). Nondestructive measurement of fruit and vegetable quality by means of NIR spectroscopy: A review. *Postharvest Biology and Technology*, *46*(2), 99–118.

O'Farrell, M., Wold, J. P., Hoy, M., Tschudi, J., & Schulerud, H. (2010). On-line fat content classification of in homogeneous pork trimmings using multispectral near infrared interactance imaging. *Journal of Near Infrared Spectroscopy*, *18*(2), 135–146.

Pedreschi, F., Segtnan, V. H., & Knutsen, S. H. (2010). On-line monitoring of fat, dry matter and acrylamide contents in potato chips using near infrared interactance and visual reflectance imaging. *Food Chemistry*, *121*(2), 616–620.

Peng, Y. K., Zhang, J., Wang, W., Li, Y. Y., Wu, J. H., Huang, H., et al. (2011). Potential prediction of the microbial spoilage of beef using spatially resolved hyperspectral scattering profiles. *Journal of Food Engineering*, *102*(2), 163–169.

Prevolnik, M., Candek-Potokar, M., & Skorjanc, D. (2010). Predicting pork water-holding capacity with NIR spectroscopy in relation to different reference methods. *Journal of Food Engineering*, *98*(3), 347–352.

Qiao, J., Wang, N., Ngadi, M. O., Gunenc, A., Monroy, M., Gariepy, C., et al. (2007). Prediction of drip-loss, pH, and color for pork using a hyperspectral imaging technique. *Meat Science*, *76*(1), 1–8.

Qin, J., Burks, T. F., Zhao, X., Niphadkar, N., & Ritenour, M. A. (2011). Multispectral detection of citrus canker using hyperspectral band selection. *Transactions of the ASABE*, *54*(6), 2331–2341.

Qin, J. W., Burks, T. F., Zhao, X. H., Niphadkar, N., & Ritenour, M. A. (2012). Development of a two-band spectral imaging system for real-time citrus canker detection. *Journal of Food Engineering*, *108*(1), 87–93.

Rajkumar, P., Wang, N., Eimasry, G., Raghavan, G. S. V., & Gariepy, Y. (2012). Studies on banana fruit quality and maturity stages using hyperspectral imaging. *Journal of Food Engineering*, *108*(1), 194–200.

Rodríguez-Pulido, F. J., Barbin, D. F., Sun, D. -W., Gordillo, B., González-Miret, M. L., & Heredia, F. J. (2013). Grape seed characterization by NIR hyperspectral imaging. *Postharvest Biology and Technology*, *76*, 74–82.

Saranwong, S., Haff, R. P., Thanapase, W., Janhiran, A., Kasemsumran, S., & Kawano, S. (2011). Short communication: A feasibility study using simplified near infrared imaging to detect fruit fly larvae in intact fruit. *Journal of Near Infrared Spectroscopy*, *19*(1), 55–60.

Serranti, S., Cesare, D., & Bonifazi, G. (2012). Hyperspectral-imaging-based techniques applied to wheat kernels characterization. *Proc. SPIE 8369, Sensing for Agriculture and Food Quality and Safety IV, Vol. 8369OT.* (pp. 83690T–83691T).

Shahin, M. A., & Symons, S. J. (2011). Detection of *Fusarium* damaged kernels in Canada Western Red Spring wheat using visible/near-infrared hyperspectral imaging and principal component analysis. *Computers and Electronics in Agriculture*, *75*(1), 107–112.

Shahin, M. A., Symons, S. J., & Hatcher, D. W. (2013). Quantification of mildew damage in soft red winter wheat based on spectral characteristics of bulk samples: A comparison of visible-near-infrared imaging and near-infrared spectroscopy. *Food and Bioprocess Technology*. http://dx.doi.org/10.1007/s11947-012-1046-8 (in press).

Singh, C. B., Jayas, D. S., Paliwal, J., & White, N. D. G. (2010a). Detection of midge-damaged wheat kernels using short-wave near-infrared hyperspectral and digital colour imaging. *Biosystems Engineering*, *105*(3), 380–387.

Singh, C. B., Jayas, D. S., Paliwal, J., & White, N. D. G. (2010b). Identification of insect-damaged wheat kernels using short-wave near-infrared hyperspectral and digital colour imaging. *Computers and Electronics in Agriculture*, *73*(2), 118–125.

Singh, C., Jayas, D., Paliwal, J., & White, N. (2012). Fungal damage detection in wheat using short-wave near-infrared hyperspectral and digital colour imaging. *International Journal of Food Properties*, *15*(1), 11–24.

Sivertsen, A. H., Heia, K., Hindberg, K., & Godtliebsen, F. (2012). Automatic nematode detection in cod fillets (*Gadus morhua* L.) by hyperspectral imaging. *Journal of Food Engineering*, *111*(4), 675–681.

Sivertsen, A. H., Heia, K., Stormo, S. K., Elvevoll, E., & Nilsen, H. (2011a). Automatic nematode detection in cod fillets (*Gadus morhua*) by transillumination hyperspectral imaging. *Journal of Food Science*, *76*(1), S77–S83.

Sivertsen, A. H., Kimiya, T., & Heia, K. (2011b). Automatic freshness assessment of cod (*Gadus morhua*) fillets by Vis/Nir spectroscopy. *Journal of Food Engineering*, *103*(3), 317–323.

Sone, I., Olsen, R. L., Sivertsen, A. H., Eilertsen, G., & Heia, K. (2012). Classification of fresh Atlantic salmon (*Salmo salar* L.) fillets stored under different atmospheres by hyperspectral imaging. *Journal of Food Engineering*, *109*(3), 482–489.

Stevik, A. M., Duun, A. S., Rustad, T., O'Farrell, M., Schulerud, H., & Ottestad, S. (2010). Ice fraction assessment by near-infrared spectroscopy enhancing automated superchilling process lines. *Journal of Food Engineering*, *100*(1), 169–177.

Sun, D. -W. (2008a). *Computer vision technology for food quality evaluation.* San Diego, California, USA: Elsevier (Academic Press).

Sun, D. -W. (2008b). *Infrared spectroscopy for food quality analysis and control.* San Diego, California, USA: Elsevier (Academic Press).

Sun, D. -W. (1999). Comparison and selection of EMC ERH isotherm equations for rice. *Journal of Stored Products Research*, *35*(3), 249–264. http://dx.doi.org/10.1016/S0022-474X(99)00009-0.

Sun, D. -W. (2010). *Hyperspectral imaging for food quality analysis and control.* San Diego, California, USA: Academic Press/Elsevier.

Sun, D. -W., & Brosnan, T. (2003). Pizza quality evaluation using computer vision - part 1 - Pizza base and sauce spread. *Journal of Food Engineering*, *57*(1), 81–89. http://dx.doi.org/10.1016/S0260-8774(02)00275-3 (Article Number: PII S0260-8774(02)00275-3).

Sun, D. -W., & Byrne, C. (1998). Selection of EMC/ERH isotherm equations for rapeseed. *Journal of Agricultural Engineering Research*, *69*(4), 307–315. http://dx.doi.org/10.1006/jaer.1997.0249.

Sun, D. -W., & Hu, Z. H. (2003). CFD simulation of coupled heat and mass transfer through porous foods during vacuum cooling process. *International Journal of Refrigeration-Revue Internationale Du Froid*, *26*(1), 19–27. http://dx.doi.org/10.1016/S0140-7007(02)00038-5 (Article Number: PII S0140-7007(02)00038-5).

Sun, D. -W., & Woods, J. L. (1993). The moisture-content relative-humidity equilibrium relationship of wheat - A review. *Drying Technology*, *11*(7), 1523–1551. http://dx.doi.org/10.1080/07373939308916918.

Sun, D. -W., & Woods, J. L. (1994a). The selection of sorption isotherm equations for wheat-based on the fitting of avaliable data. *Journal of Stored Products Research*, *30*(1), 27–43. http://dx.doi.org/10.1016/0022-474X(94)90270-4.

Sun, D. -W., & Woods, J. L. (1994b). Low-temperature moisture transfer characteristics of wheat in thin-layers. *Transactions of the Asae*, *37*(6), 1919–1926.

Sun, D. -W., & Woods, J. L. (1994c). Low-temperature moisture transfer characteristics of Barley - Thin -layers models and equilibrium isotherms. *Journal of Agricultural Engineering Research*, *59*(4), 273–283. http://dx.doi.org/10.1006/jaer.1994.1086.

Sun, D. -W., & Woods, J. L. (1997). Simulation of the heat and moisture transfer process during drying in deep grain beds. *Drying Technology*, *15*(10), 2479–2508. http://dx.doi.org/10.1080/07373939708917371.

Sun, D. -W., & Zheng, L. Y. (2006). Vacuum cooling technology for the agri-food industry: Past, present and future. *Journal of Food Engineering*, *77*(2), 203–214. http://dx.doi.org/10.1016/j.jfoodeng.2005.06.023.

Taghizadeh, M., Gowen, A. A., & O'Donnell, C. P. (2011). Comparison of hyperspectral imaging with conventional RGB imaging for quality evaluation of *Agaricus bisporus* mushrooms. *Biosystems Engineering*, *108*(2), 191–194.

Talens, P., Mora, L., Morsy, N., Barbin, D. F., ElMasry, G., & Sun, D. -W. (2013). Prediction of water and protein contents and quality classification of Spanish cooked ham using NIR hyperspectral imaging. *Journal of Food Engineering*, *117*(3), 272–280.

Tao, F. F., Peng, Y. K., Li, Y. Y., CHao, K. L., & Dhakal, S. (2012). Simultaneous determination of tenderness and *Escherichia coli* contamination of pork using hyperspectral scattering technique. *Meat Science*, *90*, 851–857.

Tao, F. F., Wang, W., Li, Y. Y., Peng, Y. K., Wu, J. H., Shan, J. J., et al. (2010). A rapid nondestructive measurement method for assessing the total plate count on chilled pork surface. *Spectroscopy and Spectral Analysis*, *30*(12), 3405–3409.

Wang, S., Huang, M., & Zhu, Q. (2012). Model fusion for prediction of apple firmness using hyperspectral scattering image. *Computers and Electronics in Agriculture*, *80*, 1–7.

Wang, B. -j, Huang, M., Zhu, Q. -b, & Wang, S. (2011a). UVE-LLE classification of apple mealiness based on hyperspectral scattering image. *Acta Photonica Sinica*, *40*(8), 1132–1136.

Wang, W., Li, C., Gitaitis, R., Tollner, E., Rains, G., & Yoon, S. C. (2010a). *Near-infrared Hyperspectral Reflectance Imaging for Early Detection of Sour Skin Disease in Vidalia Sweet Onions*. ASABE Annual International Meeting. Pittsburgh, Pennsylvania: American Society of Agricultural and Biological Engineers, St. Joseph, Michigan (Paper No. 1009106).

Wang, J., Nakano, K., Ohashi, S., Kubota, Y., Takizawa, K., & Sasaki, Y. (2011b). Detection of external insect infestations in jujube fruit using hyperspectral reflectance imaging. *Biosystems Engineering*, *108*(4), 345–351.

Wang, W., Peng, Y., Huang, H., & Wu, J. (2011c). Application of hyper-spectral imaging technique for the detection of total viable bacteria count in pork. *Sensor Letters*, *9*(3), 1024–1030.

Wang, W., Peng, Y. K., & Zhang, X. L. (2010b). Study on modeling method of total viable count of fresh pork meat based on hyperspectral imaging system. *Spectroscopy and Spectral Analysis*, *30*(2), 411–415.

Wang, L. J., & Sun, D. -W. (2001). Rapid cooling of porous and moisture foods by using vacuum cooling technology. *Trends in Food Science & Technology*, *12*(5–6), 174–184. http://dx.doi.org/10.1016/S0924-2244(01)00077-2.

Wang, L. J., & Sun, D. -W. (2002). Modelling vacuum cooling process of cooked meat - part 1: Analysis of vacuum cooling system. *International Journal of Refrigeration-Revue Internationale Du Froid*, *25*(7), 854–861. http://dx.doi.org/10.1016/S0140-7007(01)00094-9 (Article Number: PII S0140-7007(01)00094-9).

Williams, P. J., Geladi, P., Britz, T. J., & Manley, M. (2012). Investigation of fungal development in maize kernels using NIR hyperspectral imaging and multivariate data analysis. *Journal of Cereal Science*, *55*, 272–278.

Williams, P., Manley, M., Fox, G., & Geladi, P. (2010). Indirect detection of *Fusarium verticillioides* in maize (*Zea maize* L.) kernels by NIR hyperspectral imaging. *Journal of Near Infrared Spectroscopy*, *18*(1), 49–58.

Wold, J. P., Kermit, M., & Woll, A. (2010). Rapid nondestructive determination of edible meat content in crabs (*Cancer pagurus*) by near-infrared imaging spectroscopy. *Applied Spectroscopy*, *64*(7), 691–699.

Wold, J. P., O'Farrell, M., Hoy, M., & Tschudi, J. (2011). On-line determination and control of fat content in batches of beef trimmings by NIR imaging spectroscopy. *Meat Science*, *89*(3), 317–324.

Wu, D., He, H. -J., & Sun, D. -W. (2012a). Non-destructive texture analysis of farmed salmon using hyperspectral imaging technique. *Proceedings of the 3rd CIGR International Conference of Agricultural Engineering (CIGR-AgEng2012)* (Valencia, Spain).

Wu, J. H., Peng, Y. K., Chen, J. J., Wang, W., Gao, X. D., & Huang, H. (2010). Study of spatially resolved hyperspectral scattering images for assessing beef quality characteristics. *Spectroscopy and Spectral Analysis*, *30*(7), 1815–1819.

Wu, J., Peng, Y., Li, Y., Wang, W., Chen, J., & Dhakal, S. (2012b). Prediction of beef quality attributes using VIS/NIR hyperspectral scattering imaging technique. *Journal of Food Engineering*, *109*(2), 267–273.

Wu, D., Shi, H., Wang, S., He, Y., Bao, Y., & Liu, K. (2012c). Rapid prediction of moisture content of dehydrated prawns using online hyperspectral imaging system. *Analytica Chimica Acta*, *726*, 57–66.

Wu, D., & Sun, D. -W. (2012). Colour measurements by computer vision for food quality control — A review. *Trends in Food Science & Technology*, *29*(1), 5–20.

Wu, D., & Sun, D. -W. (2013a). Potential of time series-hyperspectral imaging (TS-HSI) for non-invasive determination of microbial spoilage of salmon flesh. *Talanta*, *111*, 39–46.

Wu, D., & Sun, D. -W. (2013b). Application of Visible and near infrared hyperspectral imaging for non-invasively measuring distribution of water-holding capacity in salmon flesh. *Talanta*. http://dx.doi.org/10.1016/j.talanta.2013.05.030 (in press).

Wu, D., Sun, D. -W., & He, Y. (2012d). Application of long-wave near infrared hyperspectral imaging for measurement of color distribution in salmon fillet. *Innovative Food Science & Emerging Technologies*, *16*, 361–372.

Yang, C. C., Chao, K., Kim, M. S., Chan, D. E., Early, H. L., & Bell, M. (2010). Machine vision system for on-line wholesomeness inspection of poultry carcasses. *Poultry Science*, *89*(6), 1252–1264.

Yang, C., Kim, M. S., & Chao, K. (2012a). Development and application of multispectral algorithms for defect apple inspection. *ASABE Annual International Meeting*. Dallas, Texas: The American Society of Agricultural and Biological Engineers, St. Joseph, Michigan (Paper #12133701).

Yang, C. -C., Kim, M. S., Kang, S., Cho, B. -K., Chao, K., Lefcourt, A. M., et al. (2012b). Red to far-red multispectral fluorescence image fusion for detection of fecal contamination on apples. *Journal of Food Engineering*, *108*(2), 312–319.

Yang, C. C., Kim, M. S., Kang, S., Tao, T., Chao, K., Lefcourt, A. M., et al. (2011). The development of a simple multispectral algorithm for detection of fecal contamination on apples using a hyperspectral line-scan imaging system. *Sensing and Instrumentation for Food Quality and Safety*, *5*(1), 10–18.

Yang, C. -C., Kim, M. S., Millner, P., Chao, K., & Chan, D. E. (2012c). The development of the line-scan image recognition algorithm for the detection of frass on mature tomatoes. Proc. SPIE 8369. *Sensing for Agriculture and Food Quality and Safety IV*, 836908–836908–7. http://dx.doi.org/10.1117/12.918427.

Yao, H., Hruska, Z., Kincaid, R., Brown, R., Cleveland, T., & Bhatnagar, D. (2010). Correlation and classification of single kernel fluorescence hyperspectral data with aflatoxin concentration in corn kernels inoculated with *Aspergillus flavus* spores. *Food Additives and Contaminants*, *27*(5), 701–709.

Yoon, S. C., Park, B., Lawrence, K. C., Windham, W. R., & Heitschmidt, G. W. (2011). Line-scan hyperspectral imaging system for real-time inspection of poultry carcasses with fecal material and ingesta. *Computers and Electronics in Agriculture*, *79*(2), 159–168.

Zhao, X., Burks, T. F., Qin, J., & Ritenour, M. A. (2010a). Effect of fruit harvest time on citrus canker detection using hyperspectral reflectance imaging. *Sensing and Instrumentation for Food Quality and Safety*, *4*(3), 126–135.

Zhao, J., Ouyang, Q., Chen, Q., & Wang, J. (2010b). Detection of bruise on pear by hyperspectral imaging sensor with different classification algorithms. *Sensor Letters*, *8*(4), 570–576.

Zhu, Q. B., Huang, M., Zhao, X., & Wang, S. (2013a). Wavelength selection of hyperspectral scattering image using new semi-supervised affinity propagation for prediction of firmness and soluble solid content in apples. *Food Analytical Methods*, *6*, 334–342.

Zhu, F., Zhang, D., He, Y., Liu, F., & Sun, D. -W. (2013b). Application of visible and near infrared hyperspectral imaging to differentiate between fresh and frozen-thawed fish fillets. *Food and Bioprocess Technology*. http://dx.doi.org/10.1007/s11947-012-0825-6 (in press).